EXPLORING PALLADIUM CATALYZED DECARBONYLATIVE DEHYDRATION OF CARBOXYLIC ACIDS

by

GRACE INMAN

A THESIS

Presented to the Department of Chemistry and Biochemistry
and the Robert D. Clark Honors College
in partial fulfillment of the requirements for the degree of
Bachelor of Science

May 2025

An Abstract of the Thesis of

Grace Inman for the degree of Bachelor of Science
in the Department of Chemistry to be taken May 2025

Title: Exploring Palladium Catalyzed Decarbonylative Dehydration of Carboxylic Acids

Approved: *Amanda Cook, Ph.D.*
Primary Thesis Advisor

Transition metal catalysis is an expanding field within the chemical community. Of specific interest is the identification of a renewable synthesis of alkenes for the retirement of fossil fuel consumption. Current procedures, with this end goal in mind, focus on palladium (Pd) for its catalytic properties. The focus of this research is to develop a Pd catalyst for the decarbonylative dehydration of carboxylic acids to form alkenes as precursors for synthetic molecules on an industrial level. Optimization of this catalytic system explores the impact of varying phosphine ligands, steric hindrance of the sacrificial anhydride, amount of base added, reaction temperature, and reaction rates between Pd(0) and Pd(II) sources. The aim is to tune the procedure towards the kinetically favorable terminal alkene.

Chapter I reports method and model substrate determination. This is followed by graphical representation of the calibration curve between allylbenzene and 1,3,5-trimethoxybenzene. Included is the mathematical equation used to determine yields by internal standard.

Chapter II identifies the best performing palladium pre-catalysts in the +II and 0 oxidation states for further reactivity characterizations.

Chapter III looks at varying the phosphine ligand attached to the metal center and how the increase in size and bite angle of the bidentate ligands affects the yield and selectivity of the terminal alkene.

Chapter IV compares a Pd(0) and Pd(II) species based on their initial rates, selectivity, yield, and consistency of reactivity.

Chapter V performs a temperature analysis on the reaction conditions, varying the temperature at which the reaction is completed to identify variable reactivity between Pd(0) and Pd(II) species.

Chapter VI identifies the Pd(II) species as the most consistent catalyst and varies the base loading to identify the threshold in which the catalyst and starting material activation is maximized without sacrificing selectivity or yield.

Chapter VII varies the sterics of the sacrificial anhydride to identify a trend in the selectivity and yield of the terminal alkene based on the size of catalyst intermediate structures.

Chapter VIII identifies the optimal conditions for decarbonylative dehydration of carboxylic acids that have been determined through experimental variation.

Acknowledgements

I would like to begin by thanking my incredible primary advisor, Professor Amanda Cook, for her guidance and support as I navigated the experience that is research. Through her advice and encouragement, I accepted the Presidential Undergraduate Research Scholars Fellowship, the Clarence and Lucille Dunbar Scholarship, and the Experiential Learning Scholarship which helped to fund the individual project expressed in this thesis.

And thank you to my Honors College Advisor Christopher Michlig for his excitement and engagement in learning something completely new. It was a pleasure to share my passion with him.

Additionally, I would like to thank Melanie Kascoutas for her consistent dedication to mentoring and teaching as a graduate student. Her input greatly influenced this project and helped to plant the seeds that this project grew into.

Thank you to the Cook Lab and all the members who have cheered me on, I owe them more than words can express.

Table of Contents

List of Figures

Introduction

Alkenes

Unsaturated hydrocarbons, known as alkenes, are one of the most versatile class of molecules used in the modern world. Their characteristic double bond allows for functionalization of the molecule through hydrogenation, halogenation, polymerization, and other industrially relevant reactions.[1] Common uses of alkenes include the synthesis of Styrofoam from styrene,[2] the synthesis of zinc oxide eugenol from eugenol for root canal sealing and pain control,[3] and the production of polyethylene from ethylene for packaging applications.[4] While widely applied in synthesis, alkenes, such as propylene and ethylene, are primarily sourced from nonrenewable resources such as petroleum and crude oil. Known as *crude oil distillation*, the synthesis of alkenes begins with heating crude oil to over 1000 °C and collecting the products in fractions based on their boiling points, with the lowest collected fraction being that of butane and light hydrocarbons.[5] Further fractions include jet fuel, kerosene, and diesel fuel.[5] Traditionally crude oil distillation collects saturated hydrocarbons, and these long carbon chains undergo further refinement known as *steam cracking*, breaking these chains into components that contain alkenes.[6] While synthetically useful, the production of these molecules often produces environmentally detrimental byproducts such as H_2S and CO_2.[7] Because they are so synthetically useful, alkenes are a driving factor in the need for oil fracking and crude oil distillation, with over 98% of the world's ethylene production occurring from steam cracking.[8] As such the motivation for moving to renewable resources cannot be understated, and recent interest has fallen on carboxylic acids for the derivation to alkene counterparts.

Carboxylic Acids

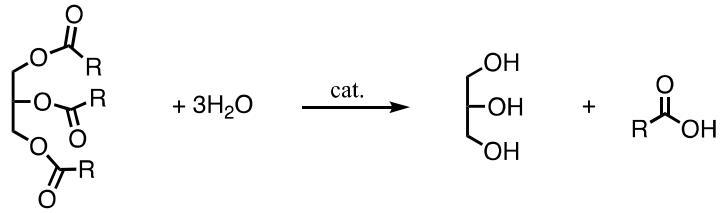

Scheme 1: Formation of carboxylic acids from triglyceride structure through hydroxylation.

Carboxylic acids are a versatile functional group that can undergo esterification, acid-base reactivity, and acyl substitution reactions for further functionalization. Long-chain carboxylic acids are formed through hydrolysis of triglycerides to produce glycerol and carboxylic acid derivatives (Scheme 1).[9] Triglycerides are naturally occurring molecules that can be found in vegetable oil and many types of fat.[10] Carboxylic acids are often found in foods and can be used as synthetic building blocks in chemical reactions. These include acetic and citric acid for vinegar and citrus tastes.[11] Further uses include acetylsalicylic acid, the anti-inflammatory drug aspirin.[11] Furthermore, these molecules are traditionally cheap and readily available, often being non-toxic and sold as supplements, such as α-lipoic acid which is marketed for anabolic support.[12] As these molecules are derived from a renewable natural resource, they are much more desirable for green chemistry applications. Therefore, chemists have been looking at the capacity for carboxylic acids to undergo decarbonylative dehydration, aiming to produce alkenes from a catalyzed decarbonylative process.

Decarbonylative Dehydration

As carboxylic acids are generally readily available and derived from natural resources, they offer an intriguing pathway to the synthesis of non-renewable resources such as alkenes. Decarbonylative dehydration, a reaction involving the loss of carbon monoxide (CO) and water, is a transition metal-catalyzed process in which a carboxylic acid loses CO and water to form a

corresponding alkene of one less carbon. While the loss of CO as a gas is entropically favorable, the amount of energy needed to pass that barrier exceeds that of a cost-efficient process, and does not happen spontaneously, leading to the necessary addition of a catalyst.[13]

Catalysis

Catalytic reactions have been used in many industrial processes for the development of energetically favorable reactions. Catalysts are consumed and reformed within the reaction vessel, acting as an intermediary organizer for the reaction to proceed through lower energy transition states in the reaction process. Early catalytic reactions were developed for the synthesis of ammonia for fertilizers using an iron catalyst and hydration of alkenes using a rhodium catalyst such as Wilkinson's catalyst.[14,15] Catalytic processes are responsible for the addition of lower energy transition states in the reaction process, decreasing the amount of energy needed for the reaction to proceed. These systems have thus been developed for a litany of reactions such as hydroformylation, hydrocyanation, hydrosilylation, and many other industrially relevant syntheses. Catalysts are further involved in the synthesis of around 80% of industrially important chemicals and are involved with an estimated $10 trillion of product development across the globe.[16] The reaction of interest for this thesis, decarbonylative dehydration, or decarboxylative elimination, is a catalytic process that causes the loss of CO or CO_2 from carboxylic acids, anhydrides, or aldehydes.[17]

Palladium-Catalyzed Decarbonylative Dehydration of Carboxylic Acids

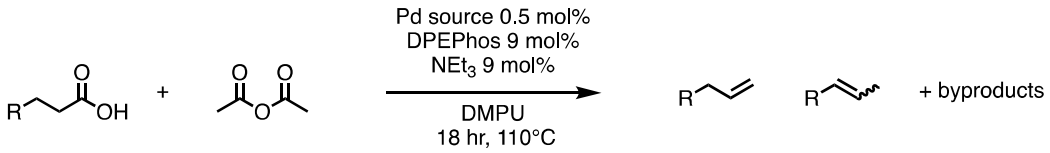

Scheme 2: Reaction conditions for decarbonylative dehydration of carboxylic acids from the Jensen Lab.

Initially developed by Joseph Miller at the Henkel Research Corporation, the decarbonylative dehydration of carboxylic acids has been investigated using a palladium catalyst to facilitate the decarbonylation of a substrate of interest.[18] Specifically looking at the work by the Jensen Lab at the University of Bergen, Norway, they have proposed a mechanism for the palladium-catalyzed decarbonylative dehydration of carboxylic acids to their linear α-olefin counterparts, based on the reaction conditions noted in the figure above.[19] Their reaction conditions (Scheme 1) have been successful in producing the terminal alkenes of long-chain carboxylic acids but have fallen short when applied to short-chain, functional group containing, carboxylic acids, a note for the extension of this work.

This catalytic system has been well studied in the literature and includes an activation of the carboxylic acid with an anhydride to form a mixed anhydride in situ. Previous studies have shown little to no reactivity if a sacrificial anhydride is not used.[20] The activation of the acid to its mixed anhydride counterpart decreases the electron density around the 3rd carbon in the chain of the mixed anhydride of component of 4-phenyl butyric acid. By decreasing the electron density from the addition of an electron-withdrawing group from the anhydride, the C–C is weakened and the Pd catalyst will more easily undergo oxidative addition into the mixed anhydride C–O bond. After oxidative addition, the C–C bond is further weakened, and the molecule undergoes decarbonylation to lose a carbon monoxide molecule into solution.

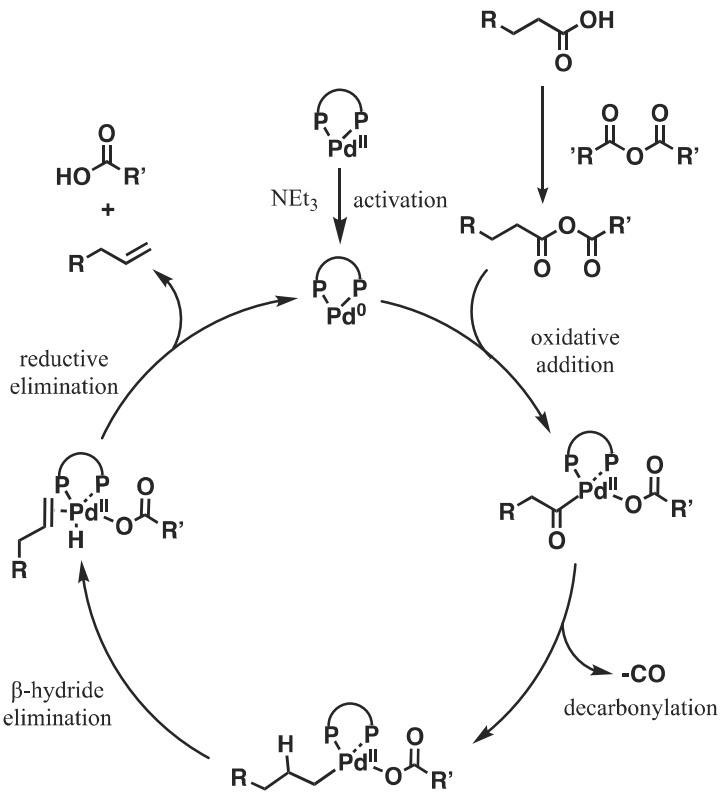

Fig 1: catalytic cycle for decarbonylative dehydration of carboxylic acids.

The catalyst then undergoes β-hydride elimination to produce the terminal alkene and an acid before reforming the Pd(0) active catalyst.[19] Studies optimizing catalyst identity, phosphine ligands, base identity and concentration, and polarity of solvent have been initiated by the Jensen Lab, concluding that reaction conditions with 9 mol % or excess of NEt_3, 9 mol % DPEPhos, a polar solvent DMPU, at 110 °C produced sufficiently high yields of alkenes from various carboxylic acids. Within these reaction conditions they identified their best pre-catalyst to be $[PdCl(cinnamyl)]_2$, a Pd(II) dimer that reacts in situ to reduce to an active Pd(0) species.[18] While not much is known about the reduction of the Pd(II) species to the Pd(0) active species, organometallic chemistry and limitations in palladium's reactivity assumes that a reactive Pd(0) species must form for the catalytic cycle to begin.[21] Pd(0) species are not usually air stable and readily oxidize to Pd(II). While identification of the chlorinated Pd(II) dimer pre-catalyst as a

well-performing Pd species expands the scope of Pd sources, it opens the door for further studies on competing palladium catalytic species. Furthermore, it's requirement for in situ reduction to Pd(0) lacks efficiency and provides motivation for the development and analysis of Pd(0) reactivity that may introduce heightened activity in the catalytic cycle. Interestingly, the investigation into the mixed anhydride identity may provide insight into the electronic behavior of the catalyst – looking at the impact on the sterics of the anhydride used and the electronic withdrawing or donating behavior of the extended carbon group. Similarly, an investigation into the bidentate phosphine ligand identity may allow for determination of catalytic trends based on the yields of terminal and internal alkenes produced. While this reaction has shown promise in synthesizing alkenes from renewable resources, it has yet to have its full potential realized through commercialization. Therefore, deeper mechanistic studies to inform and inspire catalyst improvement are warranted.

Methods

Identifying NMR peaks and data workup is included in the supplemental information for all synthesized compounds

Calibration Curve: stock solutions of 0.1195 M allylbenzene and trimethoxybenzene were created using 5 mL volumetric glassware. In increasing percentages of 10-100% allyl benzene stock solution was added to a GC vial (57, 114, 171, 228, 285, 342, 399, 457, 514, 571 uL) followed by a constant concentration of trimethoxybenzene stock solution (286 uL) and diluted with the corresponding amount of diethyl ether to afford a consistent volume of AB to TMB (950 total uL). The samples were then run on the GC under the method 30_h2_15demin_250_hold0, starting the analysis at 30 °C, ramping at 15 °C per minute until reaching 250 °C. The following retention times were afforded for each of the expected reactants and products. *allylbenzene: 6.955 $\pm$ 0.127 [min], Z β-methyl styrene: 7.247 $\pm$ 0.096 [min], E β-methyl styrene: 7.471 $\pm$ 0.100 [min], pivalic anhydride: 7.693 $\pm$ 0.131 [min], trimethoxybenzene: 9.765 $\pm$ 0.113 [min].* Data was worked up using integrated peaks on the GC traces for each compound. The peak area was used as the integral value and a plot of $\frac{\int AB}{\int TMB} vs \frac{mmol\ AB}{mmol\ TMB}$ was constructed for a calibration curve of integrated values vs concentration.

Drying 1,3-Dimethyl-3,4,5,6,-tetrahydro-2-pyrimidinone (DMPU)[22]: Desired amount of DMPU was added to a 250 mL round bottom flask followed by excess CaH (0.15 g) and allowed to stir at room temperature under positive nitrogen pressure overnight. Dried solvent was then isolated by distillation into a Schlenk flask and used as needed. Stored under nitrogen

4-phenyl butyric pivalic anhydride[23]*:* To a solution of 4-phenyl butyric acid 0.172 g, 1 equiv) in dry DCM (20 ml) at 0 °C was added pivaloyl chloride (0.209 mL, 1.7 equiv) and triethylamine (0.181 mL, 1.3 equiv) dropwise. The mixture was stirred for 1 hour at 0°C. DCM was then removed by vacuum and the residue obtained was taken up in Et_2O. The suspension was filtered through celite. Excess ether and pivaloyl chloride were removed under vacuum to yield the desired 4-phenyl butyric pivalic anhydride.

Mixed Anhydride NMR Analysis: A stir bar and 4-phenyl butyric acid (0.2 mmol, 1 equiv) were added to each 8-mL vial. The vials were capped with a septum-cap, sparged with N_2 for 15 minutes, and the anhydride (0.2 mmol, 1 equiv), DMPU (0.2 mL) and NEt_3 (20 mol%, 0.04 equiv) were added by injection with a microliter syringe. The reactions were heated to 60 °C using a pre-heated hotplate and stirred at 150 rpm for 1 hour. Reaction was monitored by ^{1}HNMR, ^{19}FNMR, and ^{13}CNMR. (Anhydrides used: acetic, pivalic, benzoic, trifluoroacetic).

Pd(COD)DQ Synthesis[24]*:* To a 100-mL round-bottom flask, equipped with a magnetic stir bar, $Pd(OAc)_2$ (224.51 mg, 1 mmol, 1 equiv), duroquinone (197.7, 1.2 mmol, 1.2 equiv). and NaOAc (246.09 mg, 3 mmol, 3 equiv) were added in air. Methanol (15 mL) and COD (552 uL, 4.5 mmol, 4.5 equiv) were subsequently added. The mixture was then stirred at room temperature for 6 h, resulting in a red homogeneous solution. The solvent was removed in vacuo to give a red residue. The residue was taken up by DCM and passed through a short silica plug, then rinsed copiously with DCM until the eluent was colorless. The combined DCM solution was concentrated to approximately 2 mL and added Et_2O to precipitate out the product. The suspension was filtered, and the solid was washed with Et_2O (×3) and dried under vacuum to yield the title compound.

Palladium Pre-Catalyst Synthesis for in situ Catalytic Trials[19]*:* A 100 mL double-necked round-bottom flask with a magnetic stir bar was filled with 12.5 mL of water and sparged with N_2 for 20 minutes. PdX_2 (0.5 mmol, 1 equiv) and KX (1 mmol, 2 equiv) were added after sparging and allowed to stir for 1 hr. After 1 hr. (R-Allyl)X (1.5 mmol, 3 equiv) compound was added and further stirred for 24 hrs. The product was then extracted with chloroform, dried over $MgSO_4$, and concentrated to yield the corresponding Pd pre-catalyst dimer. Identity and purity of the product was confirmed by ^{1}HNMR by comparison to literature reports. (X = halogen, Cl, Br; R = π-allyl ligand: cinnamyl chloride, allyl chloride, allyl bromide).

Pre-Ligated Palladium Catalyst Synthesis[25]*:* A suspension of bis(triphenylphosphino)palladium(II) chloride ($Pd(PPh_3)_2Cl_2$) (1 mmol, 0.14 g, 1 equiv) and bis(*o*-diphenylphosphinophenyl)ether (DPEPhos) (1.1 mmol, 0.161 g, 1.1 equiv) in THF (20 mL) was stirred at room temperature for 18 h. The THF was removed by vacuum and the remaining solids were filtered by suction and washed with several rinses of Et_2O. The residual solid was collected and dried in vacuo to afford the desired product as a dull yellow-green solid.

Catalytic Trials for Decarbonylative Dehydration[19]: In an 8 mL vial, a magnetic stir bar, Pd catalyst (0.003 mmol, 0.03 equiv), 4-phenyl butyric acid (0.1 mmol, 16.4 mg, 1 equiv), and DPEPhos (0.009 mmol, 4.846 mg, 0.09 equiv) were added. The vials were capped and sealed with a rubber septum and flushed with N_2 for 10 minutes. Anhydrous DMPU (2 mL), pivalic anhydride (0.2 mmol, 40.9 μL, 2 equiv), and NEt_3 in excess (20 mol%) were added by injection, measuring by difference. The reaction was then placed in an aluminum block at 110 °C and stirred at 150 rpm for 18 hrs. Once complete, an internal

standard of trimethoxybenzene was added at 0.05 M concentration per 1 mL, followed by excess Et_2O. The reaction was washed with 3 pipettefuls of NH_4Cl, H_2O, and brine. Solution was then run through a celite plug and diluted with Et_2O for GC analysis. Final yields were determined through GC integrals of trimethoxybenzene and allyl benzene.

Instrumentation:

All syntheses, manipulations, and catalytic trials were carried out under nitrogen using standard Schlenk (vacuum 10^{-2} mbar) techniques or in a nitrogen-filled glovebox unless otherwise indicated. The following solvent was used after drying and stored under nitrogen: 2,2'-(oxybis(4,1-phenylene))bis(1-phenylethane-1,2-dione) 95% (DMPU, Ambeed). The dried solvent was thereafter stored in a Schlenk flask under nitrogen. The following solvents were purchased and used without purification: toluene (Fisher Chemical), methanol (Fisher Chemical), DCM (Fisher Chemical), THF (Fisher Chemical), diethyl ether (Fisher Chemical), $CDCl_3$ (Cambridge Isotope Laboratories), d_6-DMSO (Cambridge Isotope Laboratories), d_6-benzene (Cambridge Isotope Laboratories). The following reagents were purchased and used without purification: 4-phenyl butyric acid (TCI America), 1,3,5-trimethoxybenzene (TCI America), pivalic anhydride (Acros Organics), cyclooctane (TCI America), duroquinone (TCI America), allyl chloride (Oakwood Chemicals), allyl bromide (TCI Chemicals), 3-bromo-1-propen-1-yl benzene (cinnamyl bromide, Ambeed), (3-chloropropenyl)benzene (cinnamyl chloride, Eastman Chemical Company), acetic anhydride (Fisher Chemical), benzoic anhydride (Ambeed), trifluoroacetic anhydride (Ambeed), trifluoroacetic acid (Oakwood), 6-aminocaproic acid (Aldrich), decanoic acid (Matheson Coleman & Bell), triethylamine (Aldrich), oxybis-1,4-phenylene-bisdiphenylphospine (DPEPhos, Ambeed), 1,1′-bis(diphenylphosphino)ferrocene (DPPF, Strem), 1,3-bis(phenylphosphino)propane (DPPP, Tyler Lab), triphenylphosphine (PPh_3,

Sigma-Aldrich), 4,5-bis(diphenylphosphino)-9,9-dimethylxanthene (XantPhos, TCI Chemicals), calcium hydride (Acros), $PdCl_2$ (Pressure Chemicals), $PdBr_2$ (Beantown Chemical), $Pd(OAc)_2$ trimer (Pressure Chemicals), $Pd(PPh_3)_4$ (Oakwood Chemical), $Pd[P(o\text{-}tol)_3]_2$ (Tyler Lab), $Pd(dba)_2$ (Tyler Lab). The following chemical was synthesized by accepted literature by previous lab members: $PdCl_2(PPh_3)_2$. The following chemicals were synthesized for this project according to accepted literature procedures: $PdCl_2(allyl)_2$, $PdCl_2(cinnamyl)_2$, $PdBr_2(allyl)_2$, and Pd(COD)DQ. All stock solutions were prepared by mass and were dispensed into reaction vessel by difference from syringe, as detailed in the procedure for each experiment.

General:

Nuclear magnetic resonance (NMR) spectra were collected at room temperature (298 K) unless otherwise stated on a Bruker Advance-III HD 500 NMR (499.90 MHz for ^1H; 126 MHz for ^{13}C; 471 MHz for ^{19}F). Chemical shifts are reported in parts per million (ppm, δ). ^1H and ^{13}C spectra were referenced to the residual solvent peak or tetramethylsilane (TMS) internal standard ($CDCl_3$: 1H δ = 7.26 ppm with TMS δ = 0.00 ppm, 13C δ = 77.16 ppm; C_7D_8: 1H δ = 2.08 ppm, 13C δ = 20.43 ppm, $(CD_3)_2SO$: ^1H δ = 2.5 ppm ^{13}C δ = 39.51 ppm). Peaks are characterized as follows: s (singlet), d (doublet), t (triplet), q (quartet), pent (pentet), hept (heptet), m (multiplet), br (broad), and/or ms (multiple signals). Coupling constants, *J*, are reported in Hz. For catalytic reactions, yields were determined using gas chromatography-flame ionization detector (GC) against an internal standard. GC-MS was carried out on a Shimadzu GC-2010 Plus/GCMS-QP2010 SE using a Restek Rtx®5 (Crossbond 5% diphenyl – 95% dimethyl polysiloxane; 15 m, 0.25 mm ID, 0.25 μm df) column. GC was carried out on a Thermo Fisher Trace 1300 Gas Chromatograph using a Restek Rtx®-5 (Crossbond 5% diphenyl – 95% dimethyl polysiloxane; 15 m, 0.25 mm ID, 0.25 μm df) column.

Chapter 1: Mechanistic Theory and Substrate Determination

Mechanism Exploration

The purpose of this project is to extend the functional group tolerance of the catalytic system while optimizing as many aspects of the catalytic cycle as possible. As the terminal alkene is the desired product, specific experimental variables were chosen to analyze the production of the terminal vs internal alkene based on the mechanism.

Provided the hypothesized mechanism from the Introduction (Figure 1) the system is theorized to undergo five important steps within the catalytic cycle.

Beginning with catalyst activation, the pre-catalyst ligands reductively eliminate through non-identified steps to afford the active Pd(0) catalyst with the bidentate phosphine acting as an ancillary ligand for reaction control. Therefore, we look at the following experimental conditions:

I. System dependence on the pre-catalyst oxidation state.

Catalytic activity is theorized to be higher in catalysts with lower oxidation states, therefore we explore the impact on Pd(0) and Pd(II) pre-catalysts, as well as a catalytic screening of both Pd(0) and Pd(II) sources.

II. Bidentate phosphine ligand influence on reagent orientation.

The steric and electronic effects of the bidentate ligand is studied through variation of the phosphine ligand, its steric substituents, and the chelation of the phosphine identity. This variable is tested for both Pd(0) and Pd(II) species to compare an expected inconsequential variable of pre-catalytic oxidation state and whether that impacts the catalytic activity with the phosphine ligand.

III. Thermal influence in catalytic activity.

The terminal alkene is the kinetically favored product, meaning it is likely to isomerize to more substituted carbons along the alkyl chain. As the catalyst is active at relatively high temperatures, a screening of lower temperatures is explored, comparing the activity of the best performing Pd(0) and Pd(II) catalysts. With the theory that Pd(0) catalysts may achieve better catalytic activity at lower temperatures due to its increased reactivity.

IV. Comparative loading of base for catalyst activation

The proposed mechanism highlights an activation step from the Pd(II) catalyst to the Pd(0) active catalyst, with a reducing agent, or base, specifically noted as an influence in that step. Addition of base is measured and compared to the yield of AB.

As a side reaction, the anhydride and carboxylic acid undergo an exchange reaction to afford a mixed anhydride that will enter the catalytic cycle. Introduction of a mixed anhydride causes an increase in electron-withdrawing character that weakens the internal acyl bond: By weakening that bond, the Pd catalyst can more favorably insert, and undergo oxidative addition for extended reactivity in the cycle. Therefore, the following aspects will be studied:

V. In situ formation of the mixed anhydride through NMR studies.

Formation of the mixed anhydride was studied through NMR characterization of the product based on carbonyl shifting and production of the acid counterpart. NMR studies utilized ^{13}C NMR and ^{19}F NMR.

VI. Identity of the sacrificial anhydride based on steric influence

The anhydride reflects two important roles on the catalytic cycle. Notably its electron withdrawing character and the impact on the rate of oxidative addition, followed by the steric hindrance implied by the anhydride identity. Steric hindrance is directly studied through variation of the anhydride identity.

Determination of Yield and Method Calibration

Scheme 3: Reaction conditions for model substrate determination of carboxylic acids and their corresponding alkenes

4-phenyl butyric acid, decanoic acid, and 6-aminocaproic acid were tested for viability within the reaction. Decanoic acid showed some reactivity with minimal isomerization while 6-aminocaproic acid showed no reactivity; likely due to the pK_a differences between its amine and alcohol (acid) end forming a stable ring. 4-phenyl butyric acid was chosen as the model substrate for these conditions due to its stability as well as its corresponding alkene's stability and ease of derivatization.

4-phenylbutyric acid was used in combination with its corresponding terminal alkene, allylbenzene (AB), to produce a calibration curve with respect to the internal standard 1,3,5-trimethoxybenzene (TMB) for the determination of the yield by gas chromatography (GC). The calibration curve was produced in ether and is shown in the graph below. The slope of the linear fit affords a ratio between TMB and AB that is used to calculate the percent yield of allyl benzene based on the relative integrations of the GC peaks. Retention times were confirmed by subjecting pure samples of TMB, AB, and known reagents to the noted method. Yields were calculated using the following equation:

$$\%\, AB = \frac{\int AB * mmol\ TMB}{\int TMB * mmol\ CA} * \frac{1}{2.6026} * 100$$

$\int AB$: integral of the allyl benzene curve

$\int TMB$: integral of the trimethoxybenzene curve

$mmol\ TMB$: mmol of TMB added to reaction solution

$mmol\ CA$: mmol of carboxylic acid subjected to reaction

$\frac{1}{2.6026}$: calibration curve slope ($\frac{\int AB}{\int TMB} * \frac{mmol\ AB}{mmol\ TMB}$)

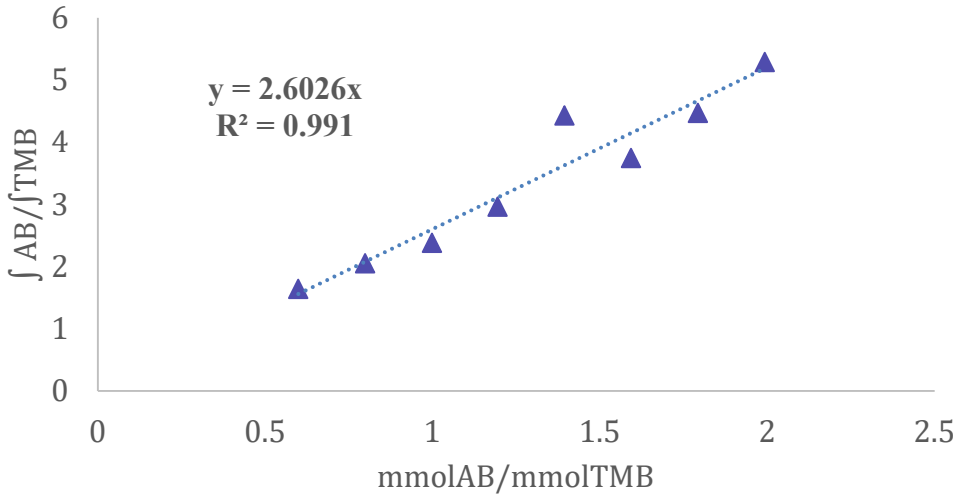

Fig 2: Calibration Curve for Allyl Benzene and 1,3,5 Trimethoxybenzene

Identification of substrate scope is limited due to the availability of carboxylic compounds in lab, the corresponding alkene of one less carbon, complexity of data work up, and time scope in which data collection was occurring.

Chapter 2: Catalyst Identification and Reactivity Trials

Catalytic reactivity depends on a litany of factors. While transition metals as atomic structures may be stable in their elemental forms, the conditions of ancillary ligands, variable solvents, temperature, time, and additional reagents expands the reactivity and applications for the metal. In this thesis Pd sources are examined following literature precedent for decarbonylative dehydration. Stemming from the reaction conditions presented in Chatterjee et al., we began our reaction optimization by examining a range of literature accepted catalysts with general trends and conclusions outlined below in subsections.[19]

Reaction Scheme for Pd Pre-Catalyst Screening

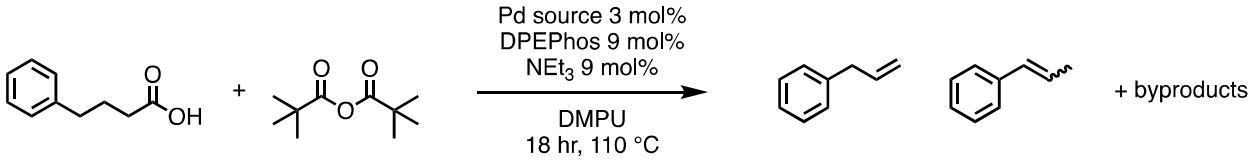

Scheme 4: Reaction scheme for the determination of best performing Pd Precatalysts.

Table 1: Catalyst Screening of Pd(0) and Pd(II) Sources

Catalysts	Pd(X)	AB %yield	bMS E %yield	bMS Z %yield	*E/Z*	Selectivity AB/bMS	Mass Balance	Std. Dev
$PdCl_2$	II	24	1	0	0	24	25	6
$PdBr_2$	II	42	1	0	0	42	43	14
$Pd(OAc)_2$	II	35	1	1	1	18	37	3
$PdCl_2(PPh_3)_2$	II	57	2	1	2	19	60	9
$[(cinnamyl)PdCl]_2$	II	29	6	3	2	3	38	2
$[(allyl)PdCl]_2$*	II	33	1	0	0	33	34	
$Pd[P(o\text{-}tol)_3]_2$	0	30	1	1	1	15	32	5

$Pd(dba)_2$	0	24	1	0	0	24	25	3
$Pd(PPh_3)_4$*	0	34	9	3	3	3	46	9
$Pd(PPh_3)_4$	0	3	0	0	0	-	3	1
Pd(COD)DQ	0	52	2	1	2	17	55	15
Pd(COD)DQ	0	4	0	0	0	-	4	1

*$PdCl_2(allyl)_2$ is reported as a single trial, $Pd(PPh_3)_4$ and Pd(COD)DQ are reported with benchtop and *glovebox reagents*

Identification of a viable group of Pd catalysts for decarbonylative dehydration stems from a variety of trends within the catalyst identity. Historically Pd catalysts offer a range of reactivity levels based on associated ligands. As this system was based off catalyst activation with a bidentate phosphine ligand, the catalyst of interest acts as the pre-catalyst. The pre-catalyst therefore defines the initial reactivity of the system and the oxidation state that the catalyst begins at.

Halogen and Pd(II) Reactivity

Table 2: Pd(0) Catalyst Screening Results

Catalysts	Pd(X)	AB %yield	bMS E %yield	bMS Z %yield	*E/Z*	Selectivity AB/bMS	Mass Balance	Std. Dev
$PdCl_2$	II	24	1	0	0	24	25	6
$PdBr_2$	II	42	1	0	0	42	43	14
$PdCl_2(PPh_3)_2$	II	57	2	1	2	19	60	9
$PdCl_2(cinnamyl)_2$	II	29	6	3	2	3	38	2
$PdCl_2(allyl)_2$	II	33	1	0	0	33	34	

Many of the Pd(II) catalysts tested contained a halogen species, imparting ionic bonds into the catalytic structure and creating a salt species. From literature precedent, utilizing XL ligands to impart steric and electronic balance was compared using allyl-based molecules. A series of trials was run using the dichloride, monochloride allyl, and monochloride cinnamyl dimers shown in Figure 2 respectively.

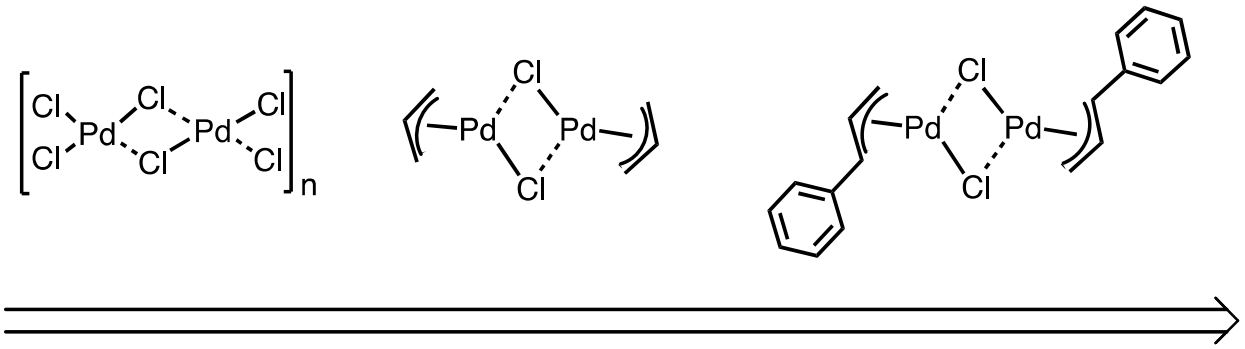

Fig 3: Increasing Sterics of the Associated Alkyl XL Ligand

Based on increasing sterics and conjugation of the pre-catalyst ligands, the stability of the dissociating allyl ligand would increase as any charge produced would now be in resonance with the phenyl ring on the cinnamyl molecule. Interestingly, the additional sterics and stability implied on the phenyl ring appears to increase the yield of the thermodynamically favored internal alkene. Therefore, by increasing the stability of the dissociating ligand, the capacity for isomerization increases. Similarly, additional stability of the dissociating ligand may impact the reduction from Pd(II) to Pd(0), with limited impact to the mass balance for the reaction.

Furthermore, $PdBr_2$ has been shown to produce the highest product yields in comparison with other Pd-halogen catalysts, but an increased variability by standard deviation. It was hypothesized that the decreased electronegativity and size of bromide may add further stereoselectivity to the catalyst, but there appears to be no viable distinction in selectivity between the $PdBr_2$ and $PdCl_2$ catalysts. There appeared minimal-to-no difference in reactivity

between the Pd-halogen and $Pd(OAc)_2$ catalysts. The best performing Pd(II) pre-catalyst thus appears to be the $PdCl_2(PPh_3)_2$ species with a yield of 57±9% and a selectivity of 19.

Pd(0) Reactivity

As a d-block metal, palladium often exists in a few oxidation states: Pd(0), Pd(II), and the less common Pd(IV) ion. The oxidation state notes the electron density around the metal center and allows chemists to predict trends in reactivity. Lower oxidation states therefore represent higher electron density and may follow a trend of higher reactivity. With higher reactivity comes instability, and Pd(0) catalysts often appear unstable under ambient, normal conditions. These catalysts, stored in air-free conditions, can access their reactivity with lower temperatures, catalyst loadings, and less additional reagents. The work of the Jensen lab identified an activation step in which the catalyst appears to reductively eliminate two of its ligands to transition from a Pd(II) catalyst into the active Pd(0) catalyst. With this understanding we hypothesized that Pd(0) catalysts would provide:

I. a faster transition into the active catalytic cycle through bypassing the reduction step

II. an increase in overall yields due to the heightened reactivity of Pd(0) species themselves.

Table 3: Pd(0) Catalyst Screening Results

Catalysts	AB %yield	bMS E %yield	bMS Z %yield	Selectivity AB/bMS	Mass Balance	Std. Dev
$Pd[P(o\text{-}tol)_3]_2$	30	1	1	15	32	5
$Pd(dba)_2$	24	1	0	21	25	3
$Pd(PPh_3)_4$	34	9	3	3	46	9
$Pd(PPh_3)_4$	3	0	0	-	3	1
Pd(COD)DQ	52	2	1	17	55	15
Pd(COD)DQ	4	0	0	-	4	1

In comparing our Pd(0) results, the highest yield appears to be Pd(COD)DQ at 52±15. With a standard deviation of 15, its reactivity is varied but it contains better selectivity of 17 compared to $Pd(PPh)_4$ at an overlapping yield deviation of 34±9% and a selectivity of 3. Comparatively Pd(COD)DQ also outperformed $Pd[P(o\text{-}tol)_3]_2$ with a yield of 30±5 and a selectivity of 15. Investigation into Pd(COD)DQ's affinity for decarbonylative dehydration of carboxylic acids is thus compared to $PdCl_2(PPh_3)_2$ as a measure of reactivity between Pd(0) and Pd(II) sources.

Table 4: Initial Reactivity for Pd(0) and Pd(II) Species

Catalysts	Pd(X)	AB %yield	bMS E %yield	bMS Z %yield	Selectivity AB/bMS	Mass Balance	Std. Dev
Pd(COD)DQ	0	52	2	1	17	55	15
$PdCl_2(PPh_3)_2$	II	57	2	1	19	60	9

Immediate comparison between initial trials of Pd(0) and Pd(II) reactivity show very similar yields of AB at 52±14% and 57±9% respectively. Their selectivity also falls under very similar ratios of 17 for our Pd(0) species and 19 for our Pd(II) species. Minimal reactivity differences prompt mechanistic investigations to compare variations between Pd(0) and Pd(II) pre-catalysts.

Chapter 3: Bidentate Phosphine Ligands and Their Bite Angle Effects

A comparison experiment was run between the Pd(0) and Pd(II) catalyst sources Pd(COD)DQ and $PdCl_2(PPh_3)_2$ to investigate the impact of the bite angle of the bidentate phosphine. This experiment aimed to encapsulate how the phosphine ligand interacted with the metal center and its role in the formation of our desired product allyl benzene. Outlined in Figure 4 the phosphine identity was varied based on increasing bite angle from tetrakis triphenyl phosphine (PPh_3, 0°), 1,3-bis(diphenylphosphino)propane (DPPP, 90°), 1,1'-bis(diphenylphosphino)ferrocene (DPPF, 100°), bis[(2-diphenylphosphino)phenyl]ether (DPEPhos, 102°) to 9,9-dimethyl-4,5-bis(diphenylphosphino)xanthene (XantPhos, 110°).

Bidentate Phosphine Ligand Series for Pd(0)

Reaction Scheme for Ligand Screening

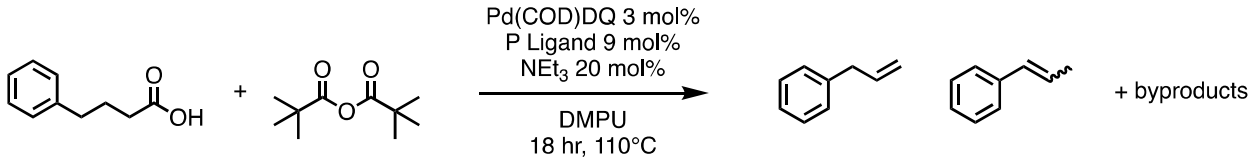

Scheme 5: Reaction conditions for phosphine ligand variations

Table 5: Phosphine Ligand Variation

P	AB %yield	bMS E %yield	bMS Z %yield	*E/Z*	Selectivity AB/bMS	Mass Balance	Std. Dev
No Phosphine	1	0	0			1	0
PPh3	2	0	0			2	1
DPPP	15	20	4	5	<1	39	9
DPPF	42	2	3	1	9	47	1
DPEPhos	51	1	1	1	26	53	3

XantPhos	50	1	0		50	51	1

When using the Pd(0) catalyst, the trend shows an increasing selectivity for the terminal alkene as the bite angle increases. Addition of no phosphine or a monodentate phosphine, PPh_3, results in a failed reaction leading to the determination that a bi or multi-dentate ligand must be used for reaction success. Monodentate and sterically limited ligands increase the variability of structures that the catalyst can access during the cycle, therefore increasing the number of reaction pathways that the catalyst can experience.

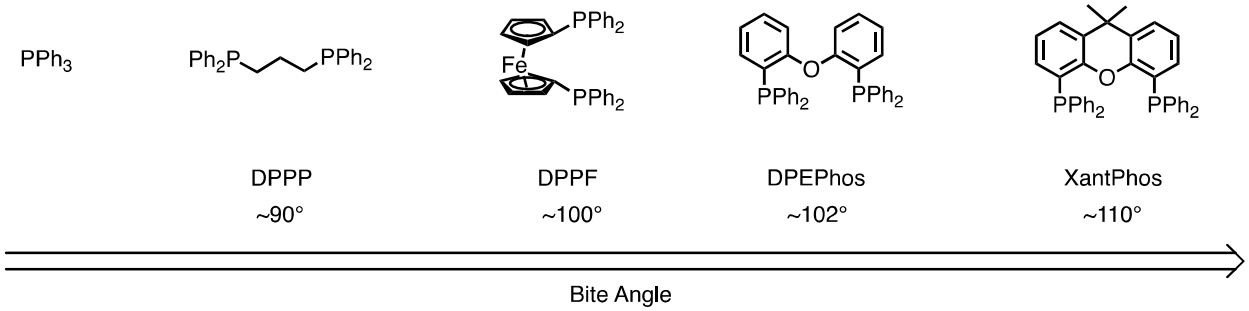

Fig 4: Increasing Size and Bite Angle of the Phosphine Ligand

By adding steric bulk and chelating activity to the ligand, the catalytic structure becomes rigid, with intermediates being locked into limited geometries. Evidence of this appears when looking at the results for DPPP, DPPF, and DPEPhos, whose structures are shown in Figure 4. DPPP with the smallest bite angle of 90° and minimal steric bulk in comparison to the ligands tested, appears to afford a mixture of products, favoring the internal alkene with a selectivity of <1. The amount of steric bulk is believed to influence the rate of reinsertion of the alkene into the catalytic cycle. As a Pd-hydride is formed from the β-hydride elimination step, and Pd-hydrides are very good at alkene isomerization, it can be concluded that the reinsertion and isomerization of the alkene is directly influenced by the bite angle and sterics of the associated phosphine ligand. Increasing the bite angle and sterics, this trend continues, and DPPF increases the

selectivity of AB:bMS to 21. The selectivity for the terminal alkene continues to grow as we look at DPEPhos and XantPhos with selectivity values of 26 and 50 respectively. Interestingly, the relationship between DPEPhos and XantPhos was expected to be relatively similar as the DPEPhos structure is derived from XantPhos.[26] Comparing the structure of the two, one can note the addition of a linked dimethyl backbone on the central carbons to the diphenyl ether. This additional linkage imparts rigidity into the backbone of the Xantphos ligand and may further inhibit reinsertion or additional active sites due to the inability for the structure to accommodate or shift in support of the interaction between the terminal alkene and the Pd-hydride. DPEPhos and XantPhos may also offer additional bonding through electron interactions from the oxygen ether and the metal center to continually maintain a stable $18e^-$ complex. The acetate ion may interchange between being bidentate and tridentate at its oxygen as the catalyst undergoes ligand association and dissociations.

Therefore, for the Pd(0) catalyst it can be concluded that the increase in bite angle and steric encumbrance directly impacts the selectivity of the product between the internal and terminal alkene. Addition of rigidity in the ligand backbone, as well as multidentate bonding behavior, may also impact product selectivity.

Bidentate Phosphine Ligand Series for Pd(II)

To extend the work done with the Pd(0) catalyst, and continue optimization, the phosphine series was repeated with the Pd(II) catalyst. The reaction vials were set up as standard, with no notable errors in procedure or work up to afford reaction failure. As the Pd(0) and Pd(II) catalysts have had relatively similar reactivity, the trend expected for the Pd(II) repeat trial was hypothesized to follow the same trend of increasing AB yield with increasing steric encumbrance and bite angle. Only DPEPhos as a ligand worked for the Pd(II) source. While human error is the

theorized source for these results, it is possible that the Pd(II) catalyst is inefficient in phosphine ligand exchange outside of the DPEPhos conditions.

Chapter 4: Time and Rates of Pd Catalyst Reactivity for Pd(0) and Pd(II) Sources

Following the identification of the two best performing catalysts, Pd(COD)DQ (0) and $PdCl_2(PPh_3)_2$ (II), a series of kinetic studies were performed to explore the hypothesis: due to the heightened reactivity of Pd(0) species, a Pd(0) pre-catalyst may more efficiently access the active catalyst state, work under sufficiently reduced temperatures, and achieve better selectivity of the kinetic product.

To begin, a time study for the proposed 18-hour reaction time was completed, using individual trials for each time point of 1, 2, 4, 8, and 18 hours, shown in Figure 5.

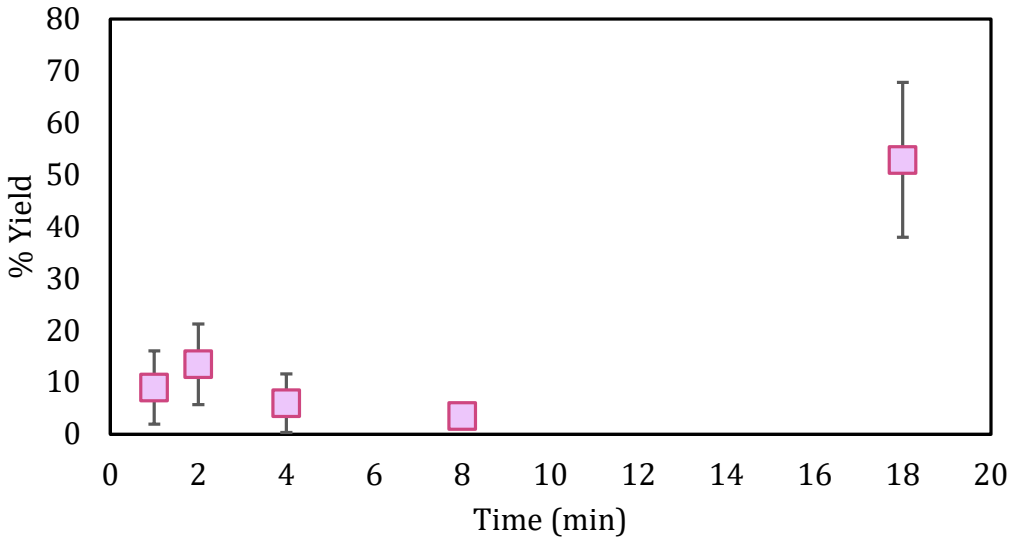

Fig 5: Pd(0) Time Study

Within the first two hours the reaction surpassed 15%, and reached completion at the 18-hour threshold, at the expected yield level of approximately 50%. When analyzing the projected yield vs time graph, the addition of large standard deviations led to the desire to study the initial rates of the Pd(0) catalyst. Looking at the first two hours as a window into ideal catalytic

behavior. The initial rates of the Pd(0) catalyst are thus shown below in Pd(0) Initial Rates and Reactivity (Figure 6).

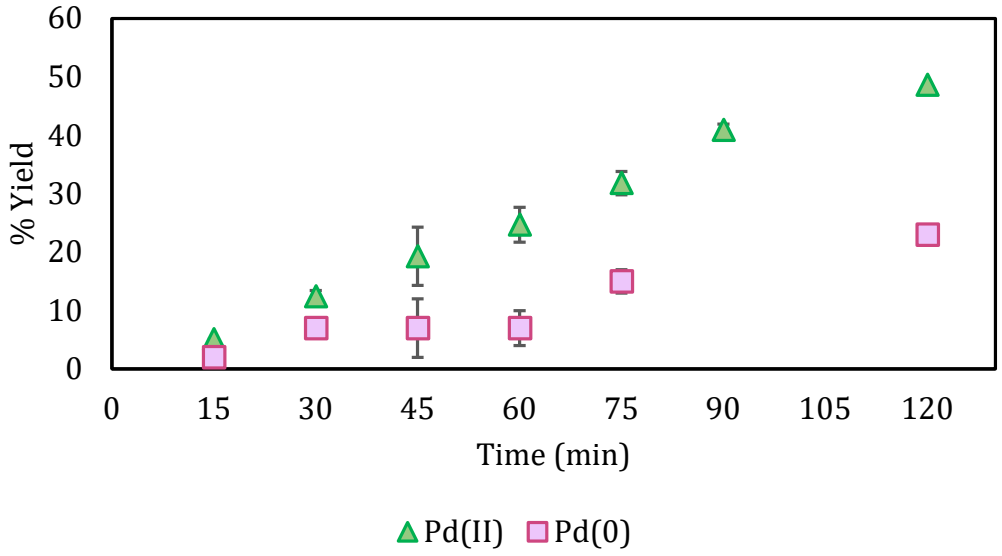

Fig 6: Pd(0) and Pd(II) Initial Rates and Reactivity

Assuming ideal conditions for catalytic activity such as limited initiation of side reactions, the 2-hour mark initially tested in the time study provided a starting point for the initial rates time window. Completing this range, the yield of the Pd(0) species, shown by the pink squares, follows an approximately linear trend with the largest variation being in trials at 45 minutes and 60 minutes. As each of these trials were set up individually the deviation present is not constant and offers insight into the instability of the reaction overall – largely due to the extensive amount of heat being used and the thermal instability of Pd(0) sources. A concurrent initial rates study was completed for the Pd(II) source shown as green triangles. It was believed that the increased reactivity of the Pd(0) species would afford a faster initial rate due to the lack of an in situ reduction from Pd(II) to Pd(0). As shown by the Pd(II) initial rates, that hypothesis is easily disproven. The initial rates of the Pd(II) catalyst under the same reaction conditions and time frame as the Pd(0) catalyst afford a more consistent linear trend for the increase of yield

over time, with the most variation occurring at the 45-minute time point. An important note is that the Pd(II) reaction reaches a maximum yield of 49%, almost matching the maximum yield found at the 18-hour time point.

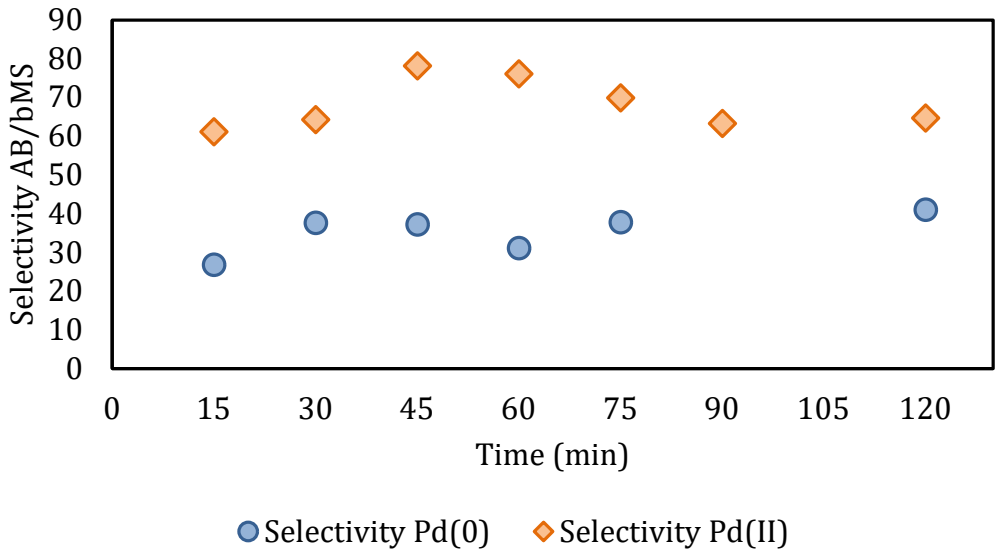

Fig 7: Selectivity Comparison Pd(0) and Pd(II)

Further comparison of the Pd(0) and Pd(II) species was carried out by contrasting the selectivity achieved within this two-hour time frame (Figure 7). Both Pd species had consistent selectivities over their respective reactions. For the Pd(0) selectivity, shown by the blue circles, the final selectivity achieved by the two-hour time point was 41, compared to the Pd(II) selectivity which ended its reaction period at a selectivity of 65. The results depicted in the graphs above are tabulat

ed below.

Table 6: Pd(0) and Pd(II) Comparative Yields and Selectivity vs Time

Time (min)	Pd(0) AB %Yield	Pd(0) Selectivity	Pd(0) Std. Dev	Pd(II) AB %Yield	Pd(II) Selectivity	Pd(II) Std. Dev
15	2	27	0	5	61	0
30	7	38	1	12	64	0
45	7	37	5	19	78	5
60	7	31	3	25	76	0
75	15	38	2	32	70	6
90				41	63	2
120	23	41	1	49	65	4

Based on the results provided, it was theorized that the Pd(0) species may be inherently unstable at these higher temperatures, leading to our next experiment where we varied the temperature of the reaction for both our Pd(0) and Pd(II) species.

Chapter 5: Temperature Dependence on Reactivity and Stability

Reaction Scheme for Temperature Dependence with Pd(0) and Pd(II) Catalysts

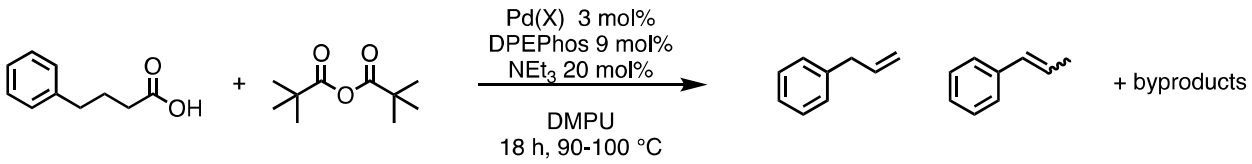

Scheme 6: Reaction conditions for temperature-based reactivity

Tests comparing the catalytic activity of the Pd(0) and Pd(II) species were conducted under the assumption that due to the Pd(0) species inherent heightened reactivity, the pre-catalyst may be able to access similar reaction yields, and possibly stabilize to a predictable catalyst at lower reaction temperatures. Four temperatures were tested, ranging from 80 °C to 110 °C. Results are tabulated and graphed below (Figure 8).

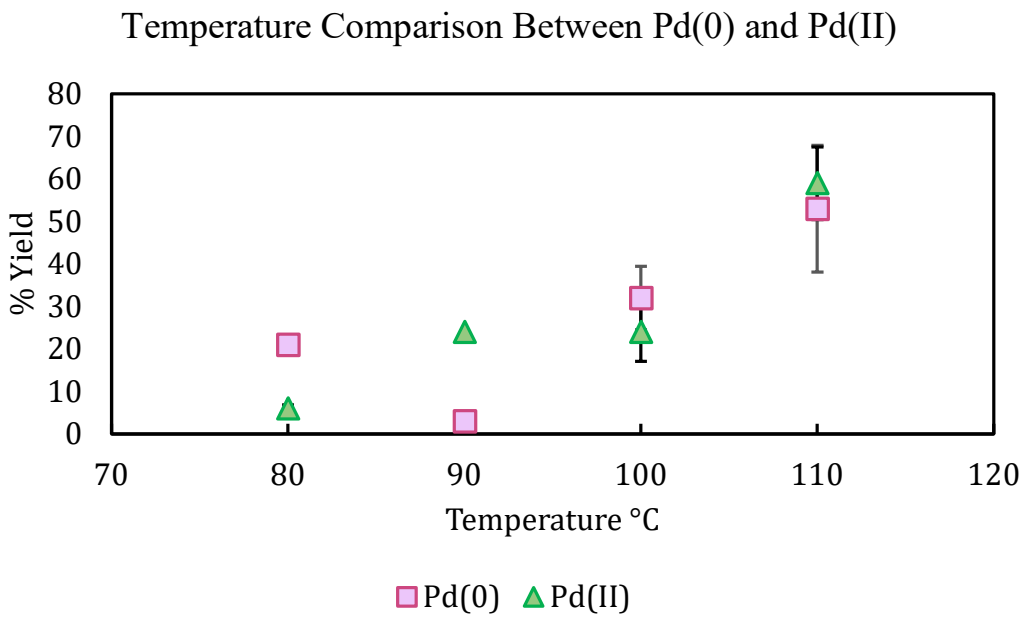

Fig 8: Temperature Comparison Between Pd(0) and Pd(II)

Table 7: Results for Pd(0) and Pd(II) Based Temperature Reactivity

Temperature (°C)	Pd(0) AB %Yield	Pd(0) Std. Dev	Pd(II) AB %Yield	Pd(II) Std. Dev
80	21	1	6	1
90	3	2	24	1
100	32	8	24	7
110	53	15	59	8

Correlation between Pd(0) and Pd(II) catalytic activity in relation to temperature appear to provide a linear and proportional relationship between competing oxidation states. As the temperature of the reaction increases the yield of the desired product increases.

At a temperature of 80 °C Pd(0) presented higher reaction yields of 21% compared to Pd(II) at 6%. At temperatures of 100 °C and 110 °C a distinct amount of variability is introduced into the catalytic system, as both the Pd(0) and Pd(II) sources have relative yield deviations of ±15% and ±8% respectively but continue to show increased yields at higher temperatures. The conclusion thus comes from the data point at 90 °C where there is minimal deviation between either Pd source but shows a distinct point in which the Pd(0) species has almost zero reactivity. This comparison to the Pd(II) source shows a difference in yield of 20% with limited explanation. As Pd(0) sources have been noted as both highly reactive and thermally unstable, it appears that the Pd(0) source is largely unreliable at any temperature and may be a poor choice in pre-catalyst for this system.

Chapter 6: Base Optimization for Reactivity

Reaction Scheme for Base Optimization: Pd(II)

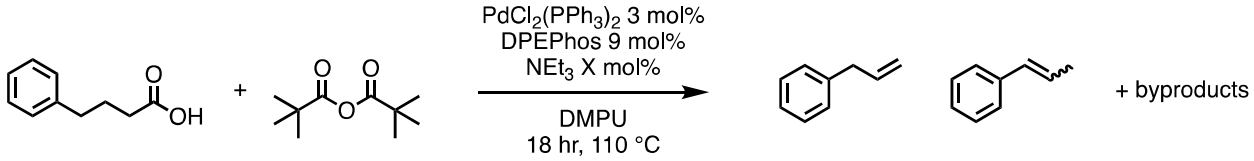

Scheme 7: Reaction conditions for base loading variations for Pd(II) species

As the Pd(0) species has been deemed unsuccessful the Pd(II) source became the focus of the optimization. Traditionally the mechanism for Pd(II) activation to Pd(0) requires a reducing agent that can facilitate the exchange of electrons required for the reduction into the catalytic cycle. Bases, like triethylamine, may act as electron donors, allowing for a redox reaction to occur and the active catalyst to be accessed. By comparing the loading percent of base for this reaction we look at the threshold of reducing agent required for catalyst activation (Figure 9).

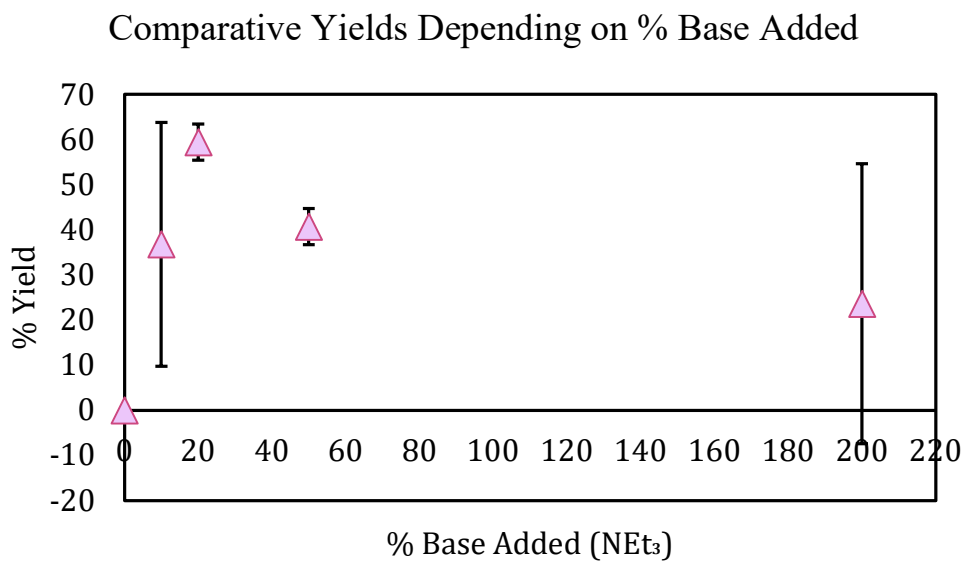

Fig 9: Comparative Yields Depending on % Base Added

Table 8: Results for Percent of Base Added Compared to Yield

Base	AB %Yield	bMS E % Yield	bMS Z % Yield	Selectivity AB/bMS	Mass Balance	Std. Dev
0%	0	0	0	0	0	0
10%	37	1	2	12	40	27
20%	59	1	2	20	62	4
50%	41	0	1		42	4
200%	24	0	0	0	24	31

At a loading of 0% the reactivity is 0 for the desired product, suggesting that no catalytic activity occurred as the catalyst was unable to reach its active state. Moving to 10% the activity increases, and we see an average yield of 37%, but a very large standard deviation, suggesting a large divergence between trials, likely from ineffective catalyst or starting material activation. As the loading is increased to 20 and 50%, we begin to hit a threshold for maximum base loading

and product yield, with 59 and 41% respectively. This threshold is confirmed by addition of excess base (200%) which appears to inhibit reactivity, likely becoming involved with side reactions between the carboxylic acid, anhydride, and additional intermediates, or inhibiting reactivity by binding with the catalyst. The base loading was then confirmed to be optimized at 20% base loading for all future trials.

Reaction Scheme for Base Optimization: Pd(0)

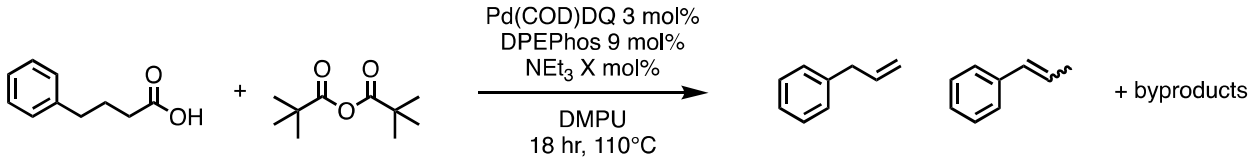

Scheme 8: Reaction conditions for base loading optimization for Pd(0) species

A similar trial was completed through studying the lack of base with the Pd(0) species. Theoretically if the catalyst was already in its required oxidation state, then the reducing agent would not be needed, and the catalyst would achieve its active state in situ with no limitations. This was tested using the Pd(0) catalyst Pd(COD)DQ and a base loading of 0%, showing no reactivity when no base was present. This attests that the base plays a secondary role in the reaction: facilitating proton transfers between the anhydride and carboxylic acid to form the reactive mixed anhydride. With no base added, the proton transfer is exceedingly limited, and minimal to no mixed anhydride is formed, resulting in unfavorable oxidative addition conditions, and no reactivity.

Chapter 7: Anhydride Optimization and Reactivity for Sterics

Sterics Investigation

Reaction Scheme for Anhydride Optimization

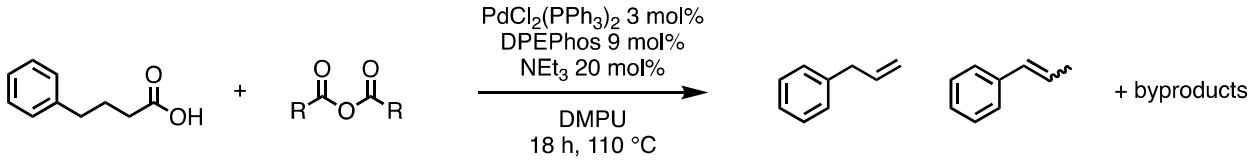

Scheme 9: Reaction conditions for anhydride variations and their reactivity

Investigation into the steric effect by the R groups on the anhydride was tested through varying anhydride identity. Three anhydrides were tested in order of increasing steric bulk: acetic anhydride, benzoic anhydride, and pivalic anhydride, and their coordinating yields and selectivity were analyzed (Figure 10).

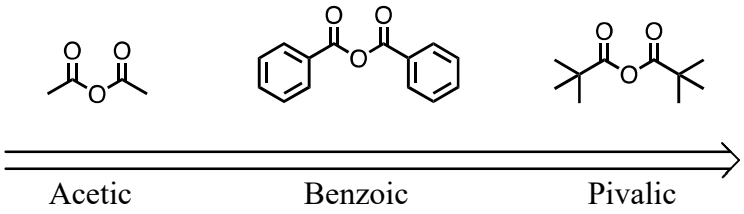

Fig 10: Varying Anhydride Identity Through Sterics

Table 9: Results for Anhydride Identity Variation

Anhydride	AB %yield	bMS E %yield	bMS Z %yield	Selectivity AB/bMS	Std. Dev of Yield	Std. Dev Selectivity
Acetic	44	3	1	21	5	1
Benzoic	44	2	1	35	5	7
Pivalic	49	1	0	49	5	1

Acetic and benzoic anhydride appeared to produce the same yield of allyl benzene at 44% with pivalic anhydride producing 49% as averages. These yields were followed by a standard deviation of ±5% placing all yields within the same range and limiting any conclusions regarding how the anhydride identity affects the yield of starting material to product. The interesting results appear under analysis of the selectivity over increasing steric bulk (Figure 11). As the smallest R group, acetic anhydride produces a selectivity of 21, there appears to be a trend where increasing the bulk of the R group thus increases the selectivity. Concretely seen in the corresponding selectivity of benzoic anhydride at 35 and pivalic anhydride at 49. Therefore, the highest selectivity occurs with the largest R group.

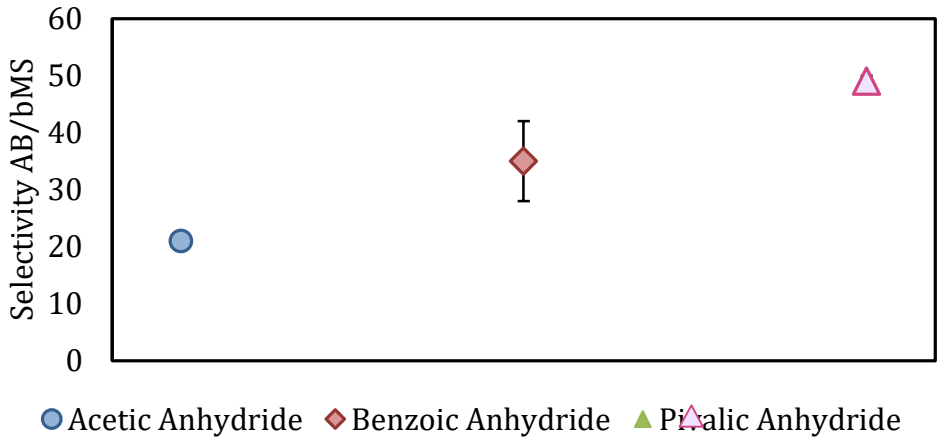

Fig 11: Increasing Steric Bulk Through Anhydride Identity

Intermediate Formation Tracked Through NMR

While the mid-range yield of the overall system continues to evade understanding, it was hypothesized that the system conditions were not fortuitous for the formation of the mixed anhydride intermediate. To study the formation of the mixed anhydride, a system of NMR studies was completed using fluorinated reagents and ^{19}F NMR analysis.

Reaction Scheme for Anhydride Optimization: ^{19}F NMR and ^{13}C NMR

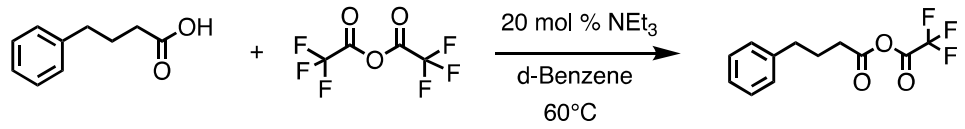

Scheme 10: Reaction conditions for fluorinated NMR analysis of mixed anhydride formation

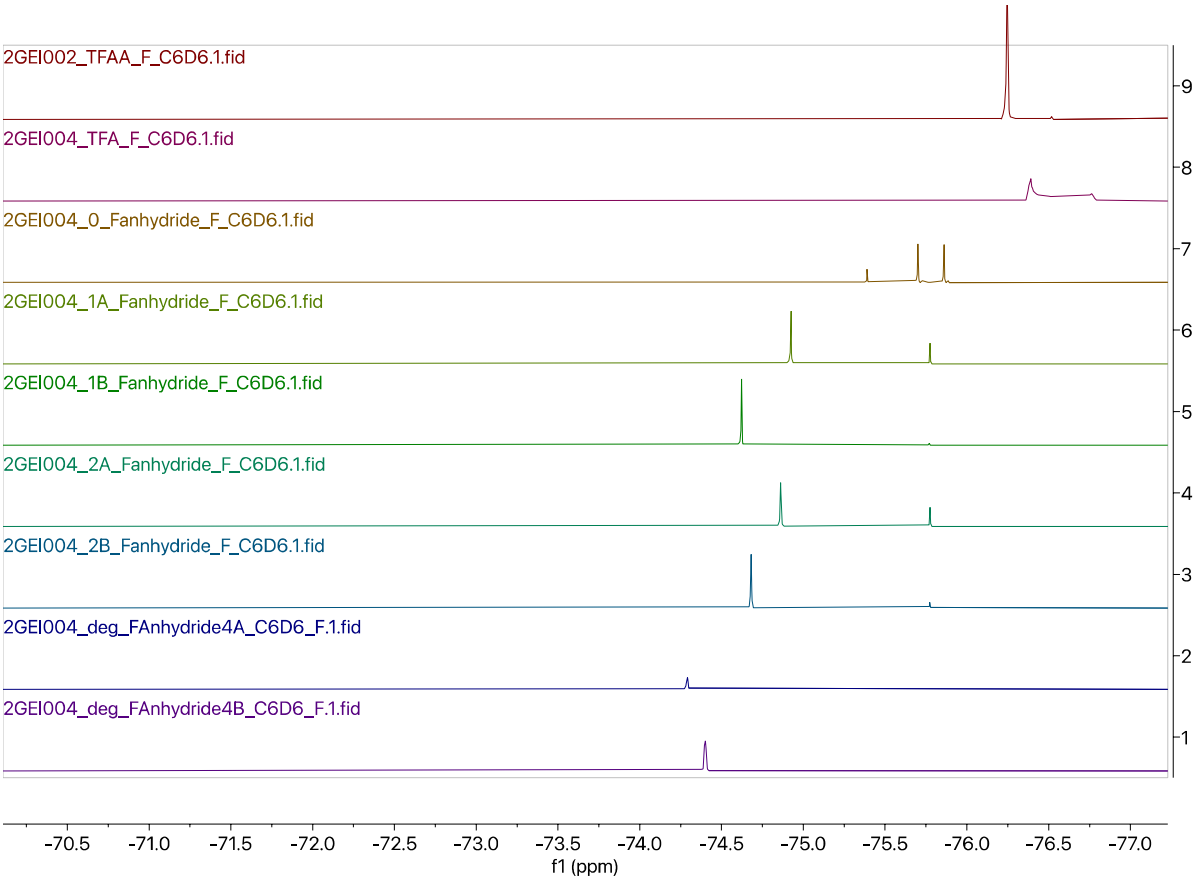

Fig 12: ^{19}F NMR for Mixed Anhydride Formation

The above ^{19}F NMR spectrum is included for result consistency, but no conclusions were able to be drawn from this specific reaction condition of 1 equivalent carboxylic acid to 2 equivalents of trifluoroacetic anhydride in a solution of d_6-benzene at 60 °C, varied through 15-minute time points over 1 hour (Figure 12).

Comparatively, when looking at the ^{13}C NMR of the fluorinated reagent reaction there is an appearance of two new peaks over the span of the hour and any intermediary peaks from the start point to the one-hour point have focused or disappeared.

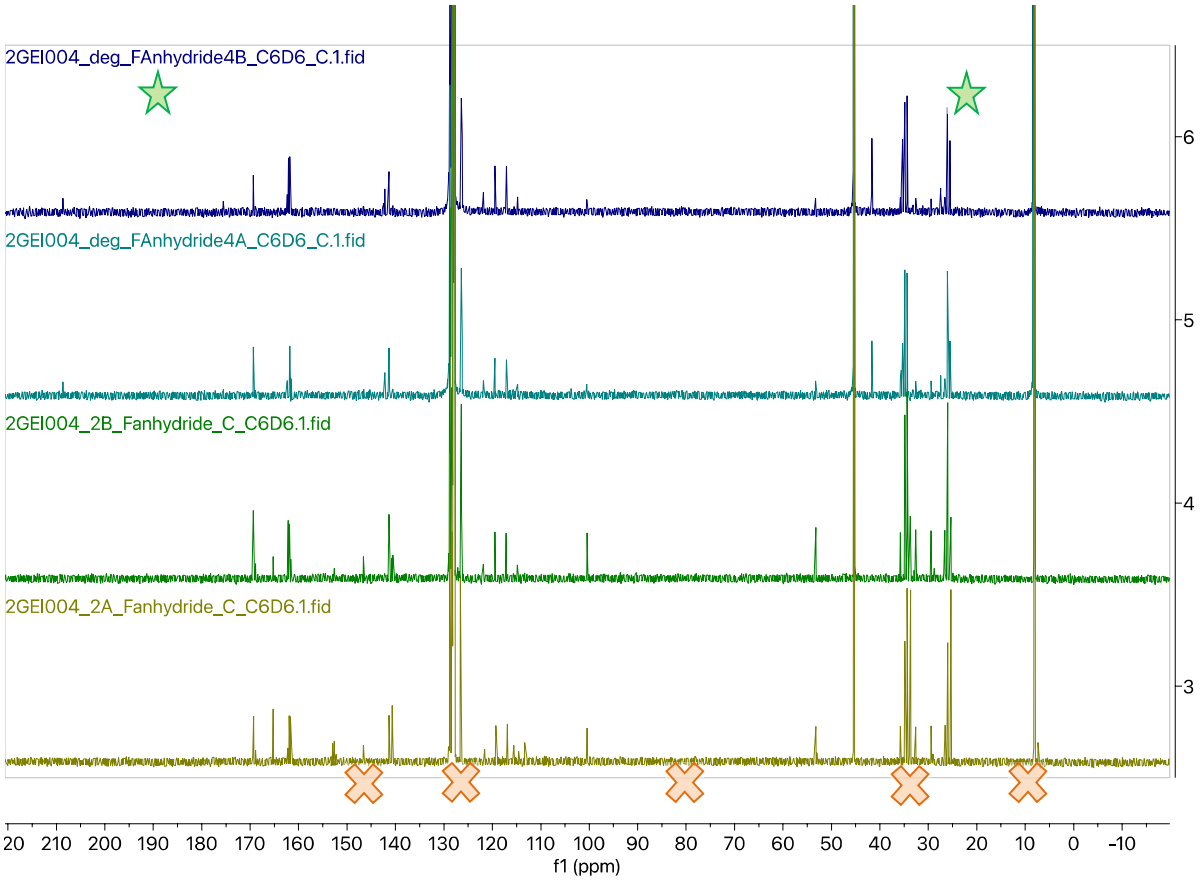

Fig 13: ^{13}C NMR for Mixed Anhydride Formation

Trial 2A and 2B are compared to Trial 4A and 4B where trial 2 encompasses 15 minutes at 60 °C and trial 4 encompasses 60 minutes at 60 °C. These trials were shown to display due to their similarities between trials compared to the other time points that lacked spectra readability.

Formation of the intermediate introduces greater deshielding of the internal carbonyl of the mixed anhydride. Therefore, a shift from the lower range of shielded atoms to higher ppms, or deshielded atoms is expected for the internal carbonyl and is highlighted by the green star over the ^{13}C NMR spectra at 208 ppm. Furthermore, as this experiment was done under qualitative measurements, the exact identity of each peak is not known, rather the appearance and

disappearance of peaks was noted and used as a measurement of if this reaction was happening (Figure 13). Therefore, peaks that appeared over time are highlighted by a green star while peaks that disappeared over time are highlighted by an orange X.

Utilizing this measure, the progress of the reaction can be measured through varying time points and the reaction, or formation of a product, is shown to be occurring at lower temperatures than the catalytic trials present. From this it can be concluded that the anhydride is being formed but lacks quantitative value for conversion of reagent to product.

Anhydride Intermediate Synthesis and Reactivity

As the mixed anhydride was now assumed to be formed in solution, the next course of action was to make the mixed anhydride on the benchtop and subject the preactivated starting material to the catalytic reaction conditions.

Synthesis of the intermediate mixed anhydride was successfully completed utilizing literature procedure noted in the methods section.

Reaction Scheme for Anhydride Optimization: ^{19}F NMR and ^{13}C NMR

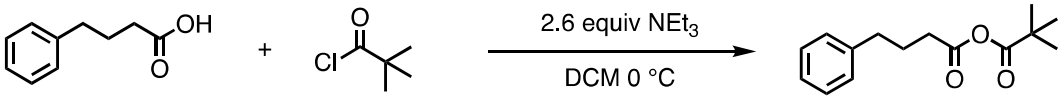

Scheme 11: Reaction conditions for mixed anhydride formation; ex situ

Obtained in relatively pure yield (>90%), without quantifying chemical identity was confirmed by ^{1}H NMR before being used in a catalytic trial, and density was determined by mass measurement with microliter syringes. One equivalent of the mixed anhydride intermediate was added, with no additional anhydride added to the system, and allowed to react under the specified conditions.

Reaction Scheme for Anhydride Optimization: ^{19}F NMR and ^{13}C NMR

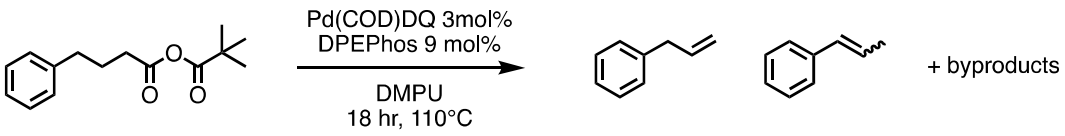

Scheme 12: Ex situ mixed anhydride catalytic trial reaction conditions

Unfortunately, ex situ formation of the mixed anhydride intermediate did not yield beneficial results to produce allyl benzene, and rather appeared to diminish reactivity. As the anhydride intermediate is pre-formed, we can assume that any side reaction between the carboxylic acid and the mixed anhydride is diminished therefore interaction with the model substrate *should* be increased.

From this notion there come two theories:

1. The slight impurities (<10%) in the anhydride intermediate most likely inhibited catalytic activity by promoting side reactions with the impurities.
2. The lack of excess anhydride may have disrupted the catalytic cycle through changes in the overall system pH. Within the system there are two bases, the anhydride and triethylamine, which may counteract reactivity of the acid produced by decarbonylative dehydration. By preforming the intermediate, any side reaction that occurs in the system between the base and the excess anhydride, or the anhydride and the carboxylic acid substrate, is decreased.

Without express experimentation to determine these ideas explicitly, there remain theories.

Chapter 8: Final Optimized Catalytic Conditions and Loadings

Optimal Reaction Scheme Based on Experimental Conditions

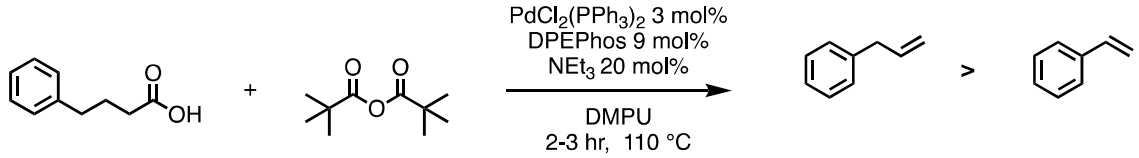

Scheme 13: Final optimized reaction conditions for decarbonylative dehydration of 4-phenyl butyric acid

Optimized Conditions

Based on the litany of experimental conditions tested, the above reaction scheme contains the best conditions for optimized reactivity between 4-phenyl butyric acid and pivalic anhydride to afford a maximum yield, and best standard deviation, of allyl benzene with 49 $\pm$ 4% yield and a selectivity of 64 $\pm$ 2. Optimization of the phosphine ligand proved a larger bite angle and increased sterics pushed selectivity to the terminal alkene. The base loading was found to reach a maximum repeatability and selectivity threshold at a 20% loading. The temperature of the reaction was maintained at 110 °C and not expected to have desirable reactivity at higher levels due to the thermal instability of the Pd catalysts tested.

Further notes look at the solvent used, as a generally toxic, polar molecule. During synthesis of the Pd pre-catalysts with allyl ligands, the analysis of each structure was completed in d_6-DMSO and $CDCl_3$ as the solubility in other deuterated organic solvents was very limited. Under this observation, and the limitations of high temperature conditions, the solvent was not varied for optimization.

While the catalyst appeared to almost complete its reactivity in 2 hours, shown in the initial rates for Pd(II), the time was not changed to provide consistency in the reactions completed prior to the kinetics study. This may be the cause for the decreased selectivity over

time as the reaction was able to stabilize and undergo alkene isomerization at increased time points.

Future Directions

The overall goal of this project was to optimize the yield of the terminal alkene, allyl benzene, from decarbonylative dehydration of its carboxylic acid precursor: 4-phenyl butyric acid. Extended studies for this reaction should include a litany of substrates with a variety of functional groups and carbon chain lengths.

Determination of electronic properties of the active catalyst should also be considered. Additional tests on the interaction with the metal center and the anhydrides – extending to electron-withdrawing groups and donating groups on the phenyl ring of benzoic anhydride. These tests may provide insight into the rate-determining step of the reaction and whether it is oxidative addition or reductive elimination based on the interactions with the activated substrate.

Further testing should also be done with other polar, high boiling point solvents, with the aim to move away from the toxic DMPU solvent. This may be expanded to include non-polar solvents but the solubility of the Pd pre-catalyst must be noted.

Catalyst loading should be varied to find the truly optimal amount for these difficult substrates, aiming to keep the loading as low as possible.

Additionally, this work may be coupled with a previously published catalyst from the Cook Lab which identifies a heterogenous Ni catalyst for alkene isomerization, changing the focus from synthesizing the terminal alkene to the internal alkene.[27]

This work should reflect an intensive approach to Palladium Catalyzed Decarbonylative Dehydration of Carboxylic Acids and may be revisited in the future.

Supplemental Information

Pd(COD)DQ

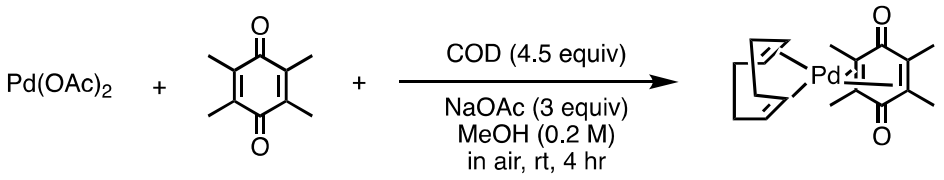

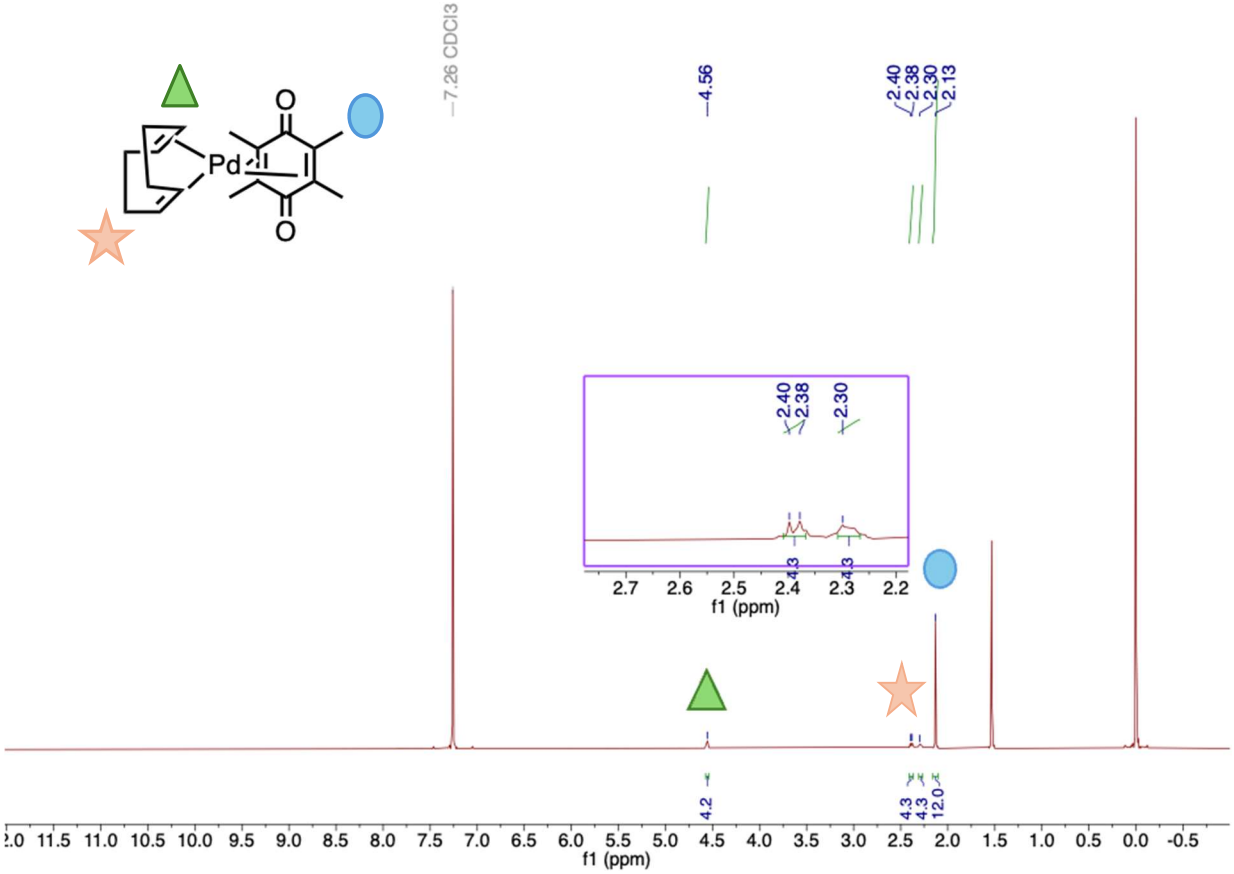

^{1}H NMR(500 MHz, $CDCl_3$) δ 4.55 (s), 2.38 (m), 2.13 (s)

[(allyl)PdCl]₂

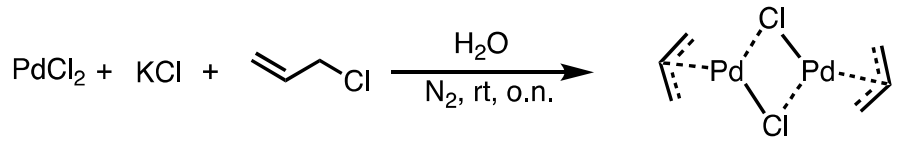

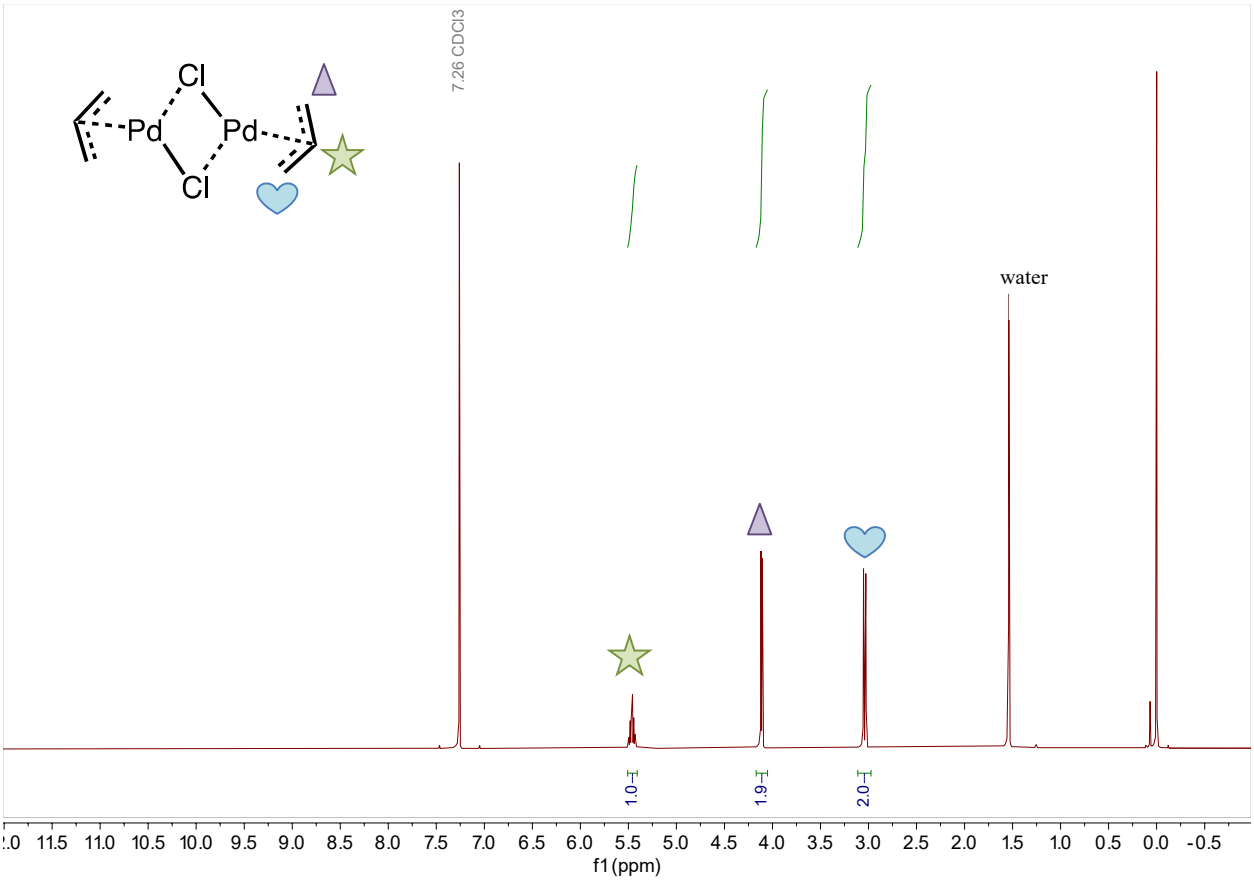

^{1}H NMR (500 MHz, $CDCl_3$) δ 5.48 (tt), 4.14 (d), 3.07 (d).

[(cinnamyl)PdCl]$_2$

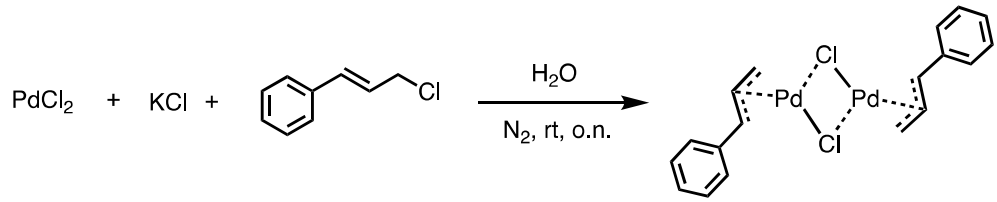

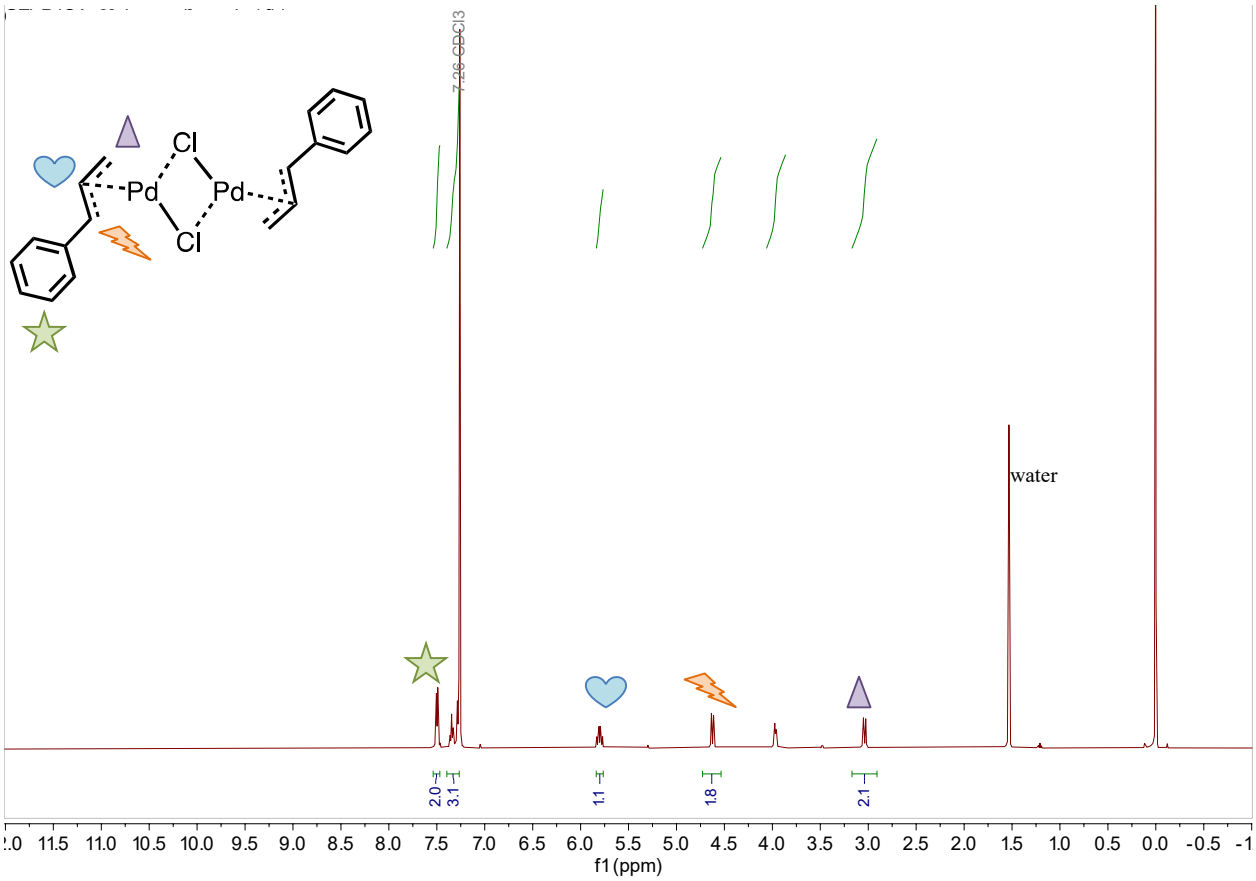

^{1}H NMR (500 MHz, $CDCl_3$) δ 7.50-7.29 (m), 5.81 (tt), 4.63 (d), 3.04 (d).

Pd(DPEPhos)Cl₂

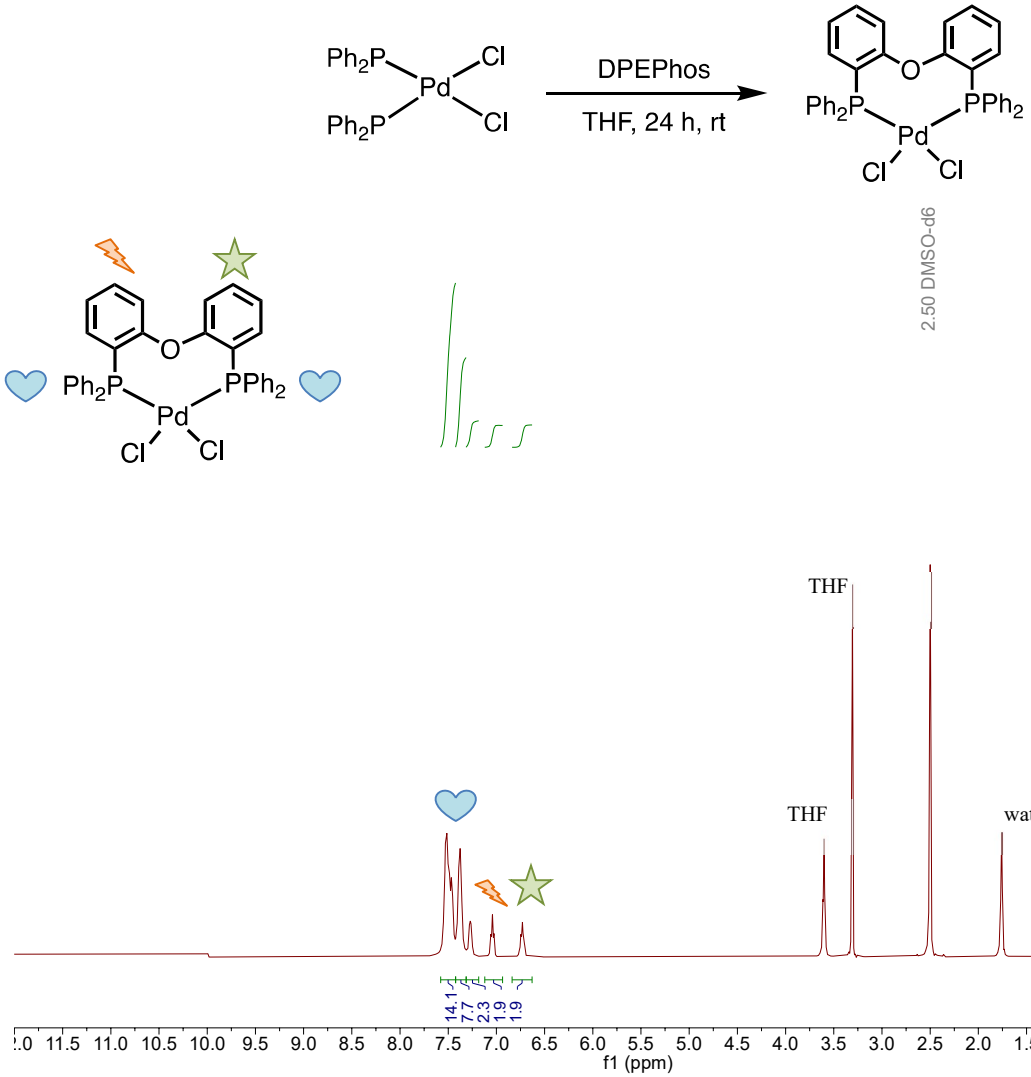

^{1}H NMR (500 MHz, DMSO) δ 7.55-7.45 (m), 7.39-7.36 (m), 7.28-7.25 (m), 7.04 (t), 6.73 (t).

4-phenylbutyric pivalic anhydride

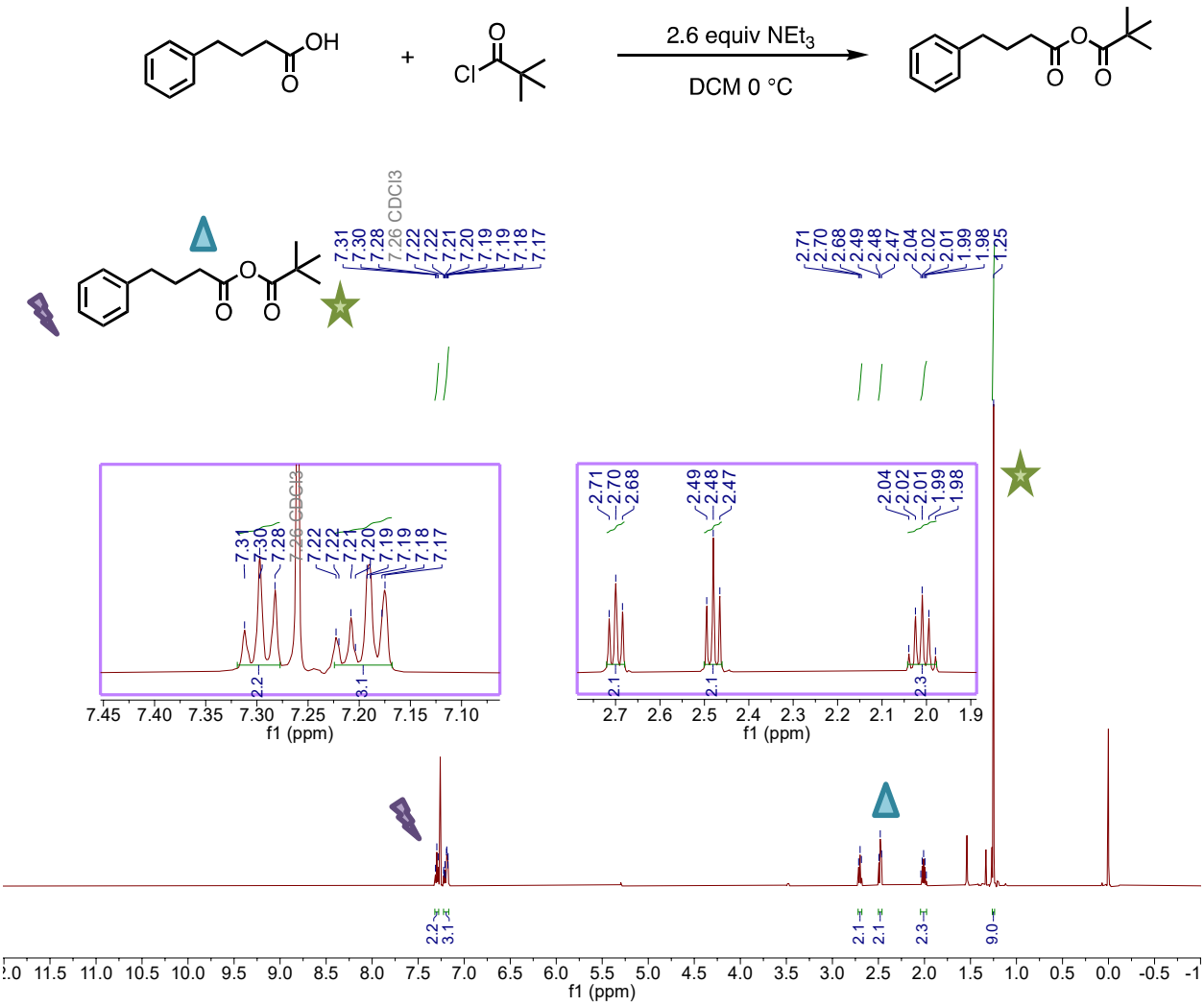

^{1}H NMR (500 MHz, $CDCl_3$) δ 7.30 (m), 7.20 (m), 2.7 (t), 2.48 (t), 2.01 (p), 1.25 (s)

1-Nonene

Model Substrate Determination: 1-nonene

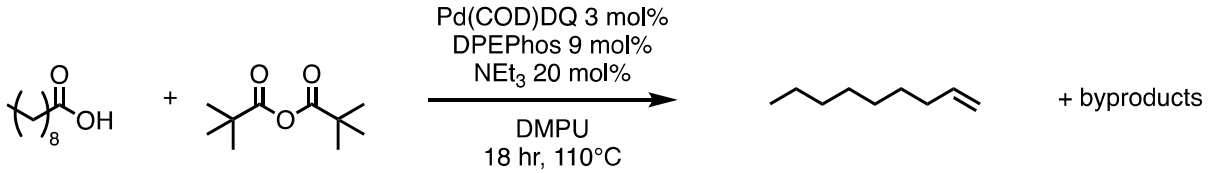

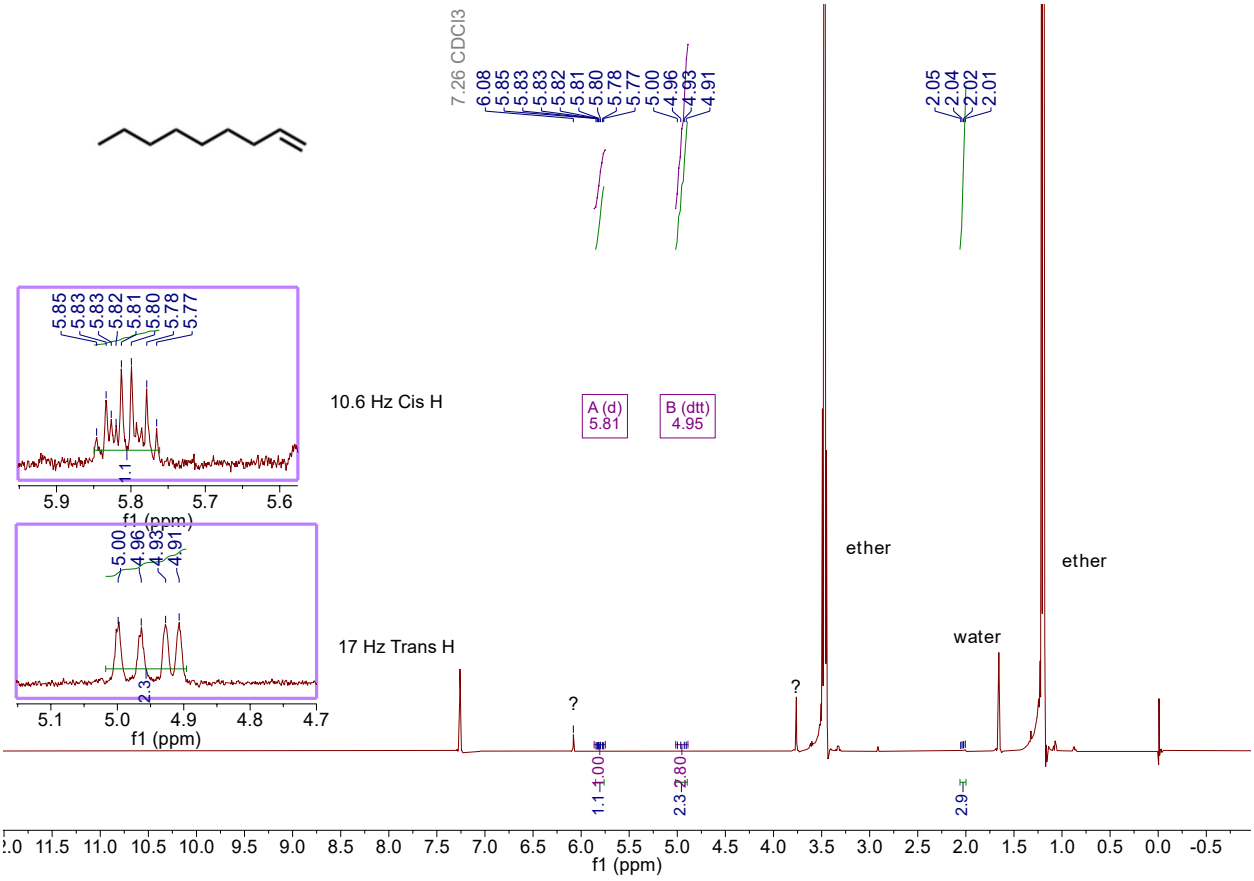

Substrate determination: evidence of cis and trans protons, no further spectra taken as decanoic acid was not the focus of this work.

4-penten-1-amine

Model Substrate Determination: 4-pente-1-amine

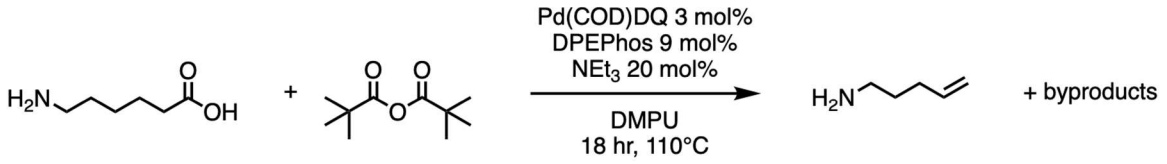

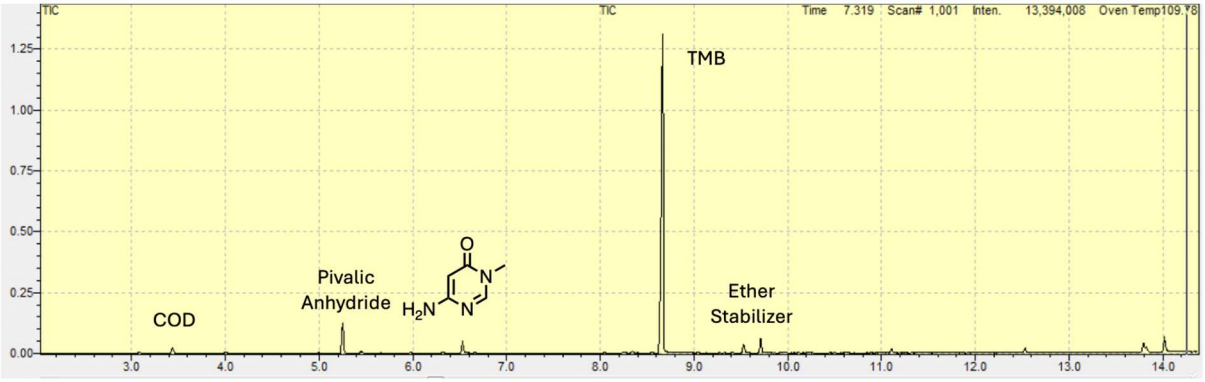

No Reactivity, based on GC-MS Analysis

Bibliography

< Alkene - an overview | ScienceDirect Topics.

Wackerly, J. Wm.; Dunne, J. F. Synthesis of Polystyrene and Molecular Weight Determination by 1H NMR End-Group Analysis. J. Chem. Educ. **2017**, 94 (11), 1790–1793.

Eugenol. https://go.drugbank.com/drugs/DB09086

Synthesis and Deconstruction of Polyethylene-type Materials | Chemical Reviews. https://pubs.acs.org/doi/10.1021/acs.chemrev.3c00587

Crude oil distillation and the definition of refinery capacity - U.S. Energy Information Administration (EIA). www.eia.gov (accessed 2024-12-16).

Stell et al. Process for Steam Cracking Heavy Hydrocarbon Feedstocks. United States Patent. **2009.** US 7,578,929 B2.

Kelland, M. A. Production Chemicals for the Oil and Gas Industry; CRC Press, 2014.

Abdulrazzaq, H. T.; Schwartz, T. J. Catalytic Conversion of Ethanol to Commodity and Specialty Chemicals. In Ethanol; Elsevier, 2019; pp 3–24.

Logan et al. Hydrolysis of Triglycerides. United States Patent. **1980**. US 4,218,386.

Libretexts. 11.3: Triglycerides- Fats and Oils. https://chem.libretexts.org/

Libretexts. 9.7: Carboxylic Acids and Esters. https://chem.libretexts.org/

Nguyen, H.; Pellegrini, M. V.; Gupta, V. Alpha-Lipoic Acid. In StatPearls; StatPearls Publishing: Treasure Island (FL), 2024.

Rouwenhorst, K. H. R.; Krzywda, P. M.; Benes, N. E.; Mul, G.; Lefferts, L. Ammonia Production Technologies. In Techno-Economic Challenges of Green Ammonia as an Energy Vector; Elsevier, 2021; pp 41–83.

John, A. Dehydrative Decarbonylation. In Organometallic Chemistry in Industry; John Wiley & Sons, Ltd, 2020; pp 283–303.

Wilkinson's catalyst. American Chemical Society. https://www.acs.org/molecule-of-the-week/archive/w/wilkinsons-catalyst.html (accessed 2024-12-16).

Ranade, V. V.; Joshi, S. S. Catalysis and Catalytic Processes. In Industrial Catalytic Processes for Fine and Specialty Chemicals; Elsevier, 2016; pp 1–14.

Decarboxylation - an overview | ScienceDirect Topics. (accessed 2024-12-16).

Miller, J. A.; Nelson, J. A.; Byrne, M. P. A highly catalytic and selective conversion of carboxylic acids to 1-alkenes of one less carbon atom. ACS Publications.

Chatterjee, A.; Hopen Eliasson, S. H.; Törnroos, K. W.; Jensen, V. R. Palladium Precatalysts for Decarbonylative Dehydration of Fatty Acids to Linear Alpha Olefins. ACS Catal. **2016**, 6 (11), 7784–7789.

Murray, R. E.; Walter, E. L.; Doll, K. M. Tandem Isomerization-Decarboxylation for Converting Alkenoic Fatty Acids into Alkenes. ACS Catal. **2014**, 4 (10), 3517–3520.

Amatore, C.; Jutand, A.; Thuilliez, A. Formation of Palladium(0) Complexes from Pd(OAc)2 and a Bidentate Phosphine Ligand (Dppp) and Their Reactivity in Oxidative Addition. Organometallics **2001**, 20 (15), 3241–3249.

Williams, D. B. G.; Lawton, M. Drying of Organic Solvents: Quantitative Evaluation of the Efficiency of Several Desiccants. J. Org. Chem. **2010**, 75 (24), 8351–8354.

Shifting-Nitroxides to Investigate Enzymatic Hydrolysis of Fatty Acids by Lipases Using Electron Paramagnetic Resonance in Turbid Media | Analytical Chemistry.

He, W.-J.; Qin, W.-Z.; Yang, S.; Ma, S.; Kim, N.; Schultz, J.; Palkowitz, M.; He, C.; Ma, A.; Schmidt, M.; Gembicky, M.; Wisniewski, S.; Engle, K. Pd(COD)(DQ): A Stable, Versatile, and Monometallic Palladium(0) Source for Organometallic Synthesis and Catalysis. ChemRxiv March 14, 2024.

Dennis, E. G.; Jeffery, D. W.; Perkins, M. V.; Smith, P. A. Pd(DPEPhos)Cl2-Catalyzed Negishi Cross-Couplings for the Formation of Biaryl and Diarylmethane Phloroglucinol Adducts. Tetrahedron **2011**, 67 (11), 2125–2131.

Gimeno, M.; Aguilera, M. C.; Fleischauer, V. E.; Brennessel, W. W.; Neidig, M. L. Effective Alkyl-Alkyl Cross-Coupling with an Iron-Xantphos Catalyst: Mechanistic and Structural Insights. Angewandte Chemie International Edition **2025**, 64 (1), e202413566.

Chang, A. S.; Kascoutas, M. A.; Valentine, Q. P.; How, K. I.; Thomas, R. M.; Cook, A. K. Alkene Isomerization Using a Heterogeneous Nickel-Hydride Catalyst. J. Am. Chem. Soc. **2024**, 146 (22), 15596–15608. https://doi.org/10.1021/jacs.4c04719.